FRA-80-5, I

REPORT NO. FRA/ORD-80/5, I

SLEEVE EXPANSION OF BOLT HOLES IN RAILROAD RAIL

Volume I - Description and Planning

D.V. Lindh
R.Q. Taylor
D.M. Rose

BOEING COMMERCIAL AIRPLANE COMPANY
P.O. Box 3707
Seattle WA 98124

FEBRUARY 1980

FINAL REPORT

Prepared for

U.S. DEPARTMENT OF TRANSPORTATION
FEDERAL RAILROAD ADMINISTRATION
Office of Research and Development
Washington DC 20590

Technical Report Documentation Page

1. Report No.	2. Government Accession No.	3. Recipient's Catalog No.
FRA/ORD-80/5,I		

4. Title and Subtitle	5. Report Date
SLEEVE EXPANSION OF BOLT HOLES IN RAILROAD RAIL Volume I, Description and Planning	Feb. 1980
	6. Performing Organization Code
7. Author(s) D.V. Lindh, R.Q. Taylor, and D.M. Rose	8. Performing Organization Report No. DOT-TSC-FRA-80-5, I
9. Performing Organization Name and Address Boeing Commercial Airplane Company* P.O. Box 3707 Seattle WA 98124	10. Work Unit No. (TRAIS) RR019/R0323
	11. Contract or Grant No. DOT-TSC-1048-1
12. Sponsoring Agency Name and Address U.S. Department of Transportation Federal Railroad Administration Office of Research and Development Washington DC 20590	13. Type of Report and Period Covered Final Report July 1975-Aug. 1977
	14. Sponsoring Agency Code

15. Supplementary Notes

*Under contract to: U.S. Department of Transportation
Research and Special Programs Administration
Transportation Systems Center
Cambridge MA 02142

16. Abstract

The most predominant failure mode of rails with bolt joints is a web crack initiating at the rail bolt hole. This failure mode is of a classical fatigue nature induced by web stress concentration around the bolt hole. This program was conducted to apply a metal-working process to the rail bolt hole to reduce the effect of such stress concentration and to demonstrate the effectiveness of the technique.

Using a process known as cold hole expansion, common to the aircraft industry, where the bolt hole is expanded to the point of plastic deformation, a residual compressive stress of both radial and tangential components is formed around the bolt hole. The compressive stress developed effectively reduces the failure-initiating stress concentration at the bolt hole.

The effectiveness of the cold-expansion process as applied to rail was demonstrated by comparison fatigue testing of both cold-expanded (CE) and non-cold-expanded (NCE) specimens. Laboratory tests indicated that life improvement for CE specimens was such that web or head failures would be the predominant failure mode, rather than CE bolt holes. The test results were statistically analyzed, indicating a factor of 10 or greater improvement in rail life due to reduction in bolt-hole failure could be anticipated.

Experimental equipment was adapted to apply cold hole expansion to an 8.5 mile test section of track in commercial service. Evaluation of this field test is continuing.

17. Key Words	18. Distribution Statement
Cold expansion, Sleeve, Crack, Fatigue, Mandrel, Rail bolt hole	DOCUMENT IS AVAILABLE TO THE PUBLIC THROUGH THE NATIONAL TECHNICAL INFORMATION SERVICE, SPRINGFIELD, VIRGINIA 22161

19. Security Classif. (of this report)	20. Security Classif. (of this page)	21. No. of Pages	22. Price
Unclassified	Unclassified	76	

Form DOT F 1700.7 (8-72) Reproduction of completed page authorized

PREFACE

This document is Volume I of a three-volume series. Volume II defines process parameters and outlines procedures for process control of the sleeve-expansion process. Volume III reports the results of a field experiment to evaluate the sleeve-expansion process and the results of three associated experiments:

- Studies on the effect of negative fatigue ratio (reverse bending) on rail sections with sleeve-expanded bolt holes

- Investigation of flaw growth in vacuum

- Life of flash-weld rail joints fabricated from uncropped rails with cold-expanded and non-cold-expanded holes.

The authors are grateful to the following individuals and organizations who contributed to this program: Mr. W. Larson, who directed the laboratory fatigue tests; the Industrial Wire and Metal Forming Company, who developed rail-cold-expansion equipment; and the Union Pacific Railroad Company, specifically Mr. R. Brown and Mr. D. Banghart, for their cooperation in the field experiment and for providing rail-failure data.

METRIC CONVERSION FACTORS

Approximate Conversions to Metric Measures

Symbol	When You Know	Multiply by	To Find	Symbol
		LENGTH		
in	inches	*2.5	centimeters	cm
ft	feet	30	centimeters	cm
yd	yards	0.9	meters	m
mi	miles	1.6	kilometers	km
		AREA		
in^2	square inches	6.5	square centimeters	cm^2
ft^2	square feet	0.09	square meters	m^2
yd^2	square yards	0.8	square meters	m^2
mi^2	square miles	2.6	square kilometers	km^2
	acres	0.4	hectares	ha
		MASS (weight)		
oz	ounces	28	grams	g
lb	pounds	0.45	kilograms	kg
	short tons (2000 lb)	0.9	tonnes	t
		VOLUME		
tsp	teaspoons	5	milliliters	ml
Tbsp	tablespoons	15	milliliters	ml
fl oz	fluid ounces	30	milliliters	ml
c	cups	0.24	liters	l
pt	pints	0.47	liters	l
qt	quarts	0.95	liters	l
gal	gallons	3.8	liters	l
ft^3	cubic feet	0.03	cubic meters	m^3
yd^3	cubic yards	0.76	cubic meters	m^3
		TEMPERATURE (exact)		
°F	Fahrenheit temperature	5/9 (after subtracting 32)	Celsius temperature	°C

*1 in = 2.54 (exactly). For other exact conversions and more detailed tables, see NBS Misc. Publ. 286, Units of Weights and Measures, Price $2.25, SD Catalog No. C13.10:286.

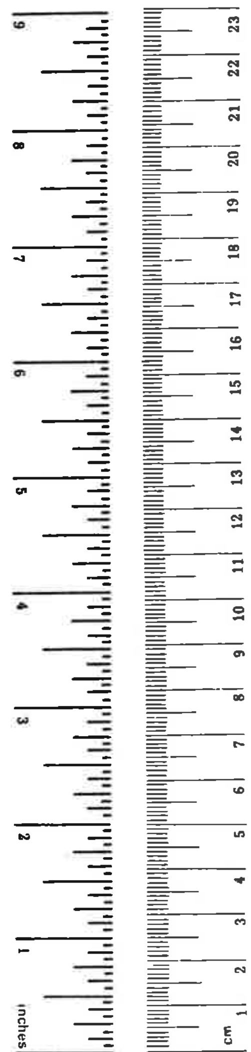

Approximate Conversions from Metric Measures

Symbol	When You Know	Multiply by	To Find	Symbol
		LENGTH		
mm	millimeters	0.04	inches	in
cm	centimeters	0.4	inches	in
m	meters	3.3	feet	ft
m	meters	1.1	yards	yd
km	kilometers	0.6	miles	mi
		AREA		
cm^2	square centimeters	0.16	square inches	in^2
m^2	square meters	1.2	square yards	yd^2
km^2	square kilometers	0.4	square miles	mi^2
ha	hectares (10,000 m^2)	2.5	acres	
		MASS (weight)		
g	grams	0.035	ounces	oz
kg	kilograms	2.2	pounds	lb
t	tonnes (1000 kg)	1.1	short tons	
		VOLUME		
ml	milliliters	0.03	fluid ounces	fl oz
l	liters	2.1	pints	pt
l	liters	1.06	quarts	qt
l	liters	0.26	gallons	gal
m^3	cubic meters	35	cubic feet	ft^3
m^3	cubic meters	1.3	cubic yards	yd^3
		TEMPERATURE (exact)		
°C	Celsius temperature	9/5 (then add 32)	Fahrenheit temperature	°F

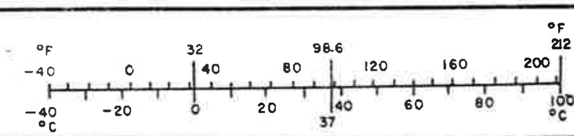

CONTENTS

CONTENTS (Concluded)

FIGURES

TABLES

ABBREVIATIONS AND SYMBOLS

AISI	American Iron and Steel Institute
C	carbon
CE	cold expanded
cfm	cubic feet per minute
Cr	chromium
Cu	copper
e	elongation
FRA	Federal Railroad Administration
Hz	hertz
ksi	kips per square inch
lb/yd	pounds per yard
Mn	manganese
Mo	molybdenum
MP	milepost
NCE	non-cold expanded
Ni	nickel
P	phosphorus
psi	pounds per square inch
R	minimum stress/maximum stress (fatigue ratio)
RC_{60}	hardness—Rockwell C scale
RE	rail section code

ABBREVIATIONS AND SYMBOLS (Concluded)

S	sulfur
Si	silicon
S-N	stress level vs number of cycles to failure
UTS	ultimate tensile strength
V	vanadium
YTS	yield tensile strength
℄	centerline
^{o}F	degrees fahrenheit

1. INTRODUCTION

Frequency of occurrence of in-service-railroad rail failures bears a direct relationship to the safety and reliability of the U.S. rail network. Data compiled by the National Transportation Safety Board (ref 1) identify broken rails as significant cause of rail replacement and further project that incidence of in-service rail fracture will increase in the future. Further analysis of statistics identifies the portion of rail enclosed by the joint bar as the most likely location for fracture, and the bolt hole as one of the most frequently encountered origins for fracture. This problem is not unique to a specific railroad, geographic location, or even country (ref 2), but is a recognized problem worldwide.

The cracks originating from bolt holes are the result of shear stress that develops in the rail end when the joint bar transmits the bending moment across the joint through concentrated point contact at the rail and at the end of the joint bar (fig. 1). This condition occurs whenever the joint bar becomes loose or, on installation, was not nested correctly between the head and flange of the rail. The shear stress is then magnified by the stress concentration effect of the bolt hole and corrosion pits that may be present.

The problem of bolt-hole cracking is not unique to the railroad industry. Aircraft manufacturers have been faced with this problem as a result of their need to minimize weight. Extensive studies have been conducted to overcome or minimize hole-associated cracking, and quite dramatic improvements have been realized and applied to jet aircraft in use today throughout the world. Improved resistance to bolt-hole fatigue cracking has been achieved by two methods, prestressing of the hole, and mechanically working the hole to develop a residual compressive stress.

Prestressing has been accomplished by insertion of an interference-fit fastener. This technique is normally applied to permanent installations that are not intended to be disassembled during the life of the structure. This technique would not lend itself to rail joints.

Comprehensive residual stresses can be developed by plastically deforming the metal immediately adjacent the hole so that it is placed in compression by reaction of the metal further removed from the edge of the hole. Three manufacturing methods are currently employed: cold expansion of the hole diameter by a removable mandrel, cold expansion of the hole diameter by a squeeze-expanded soft-metal rivet that remains permanently in the hole (the action of riveting develops a compressive stress in the hole area), and pad coining the metal adjacent to the hole. Of the three methods for inducing compressive stress, the use of a squeeze rivet would not be applicable to rail joints because of its permanent nature; however, cold expansion and pad coining would not affect ease of disassembly in the field.

---

[1] *Broken Rails: A Major Cause of Train Accidents*, NTSB RSS-74-1, January 1974.

[2] Wise, S., et al., *The Strength of Railroad Rails with Particular Reference to Rail Joints*, Proc. Inst. Mech. Engrs., 174(9), pp 371–407, 1960.

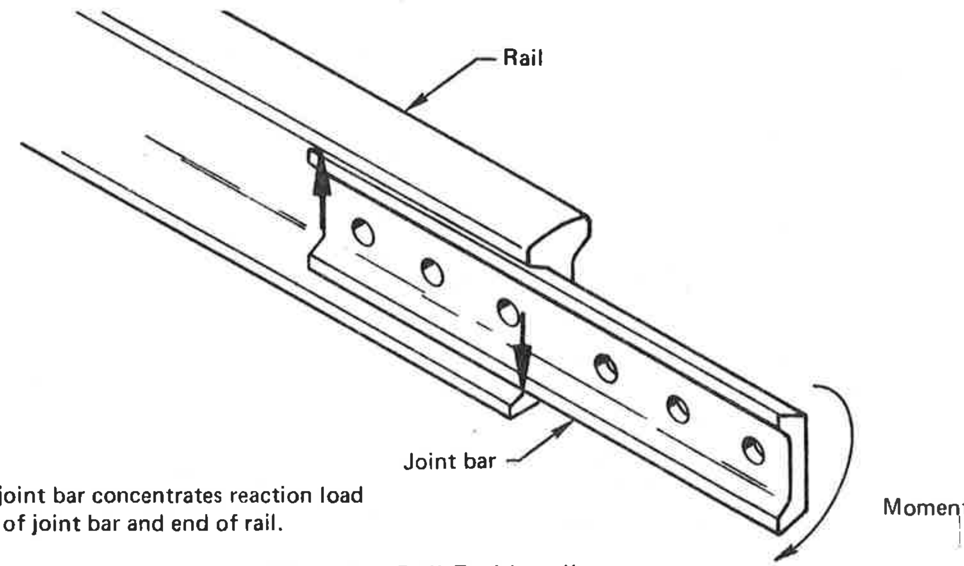

Note: Loose joint bar concentrates reaction load at end of joint bar and end of rail.

Figure 1.—Rail End Loading

Cold expansion has been investigated for fatigue improvement in Great Britain (ref 3), to a more limited extent in Belgium, and in the United States. The experimental work in Great Britain used a mandrel consisting of several spheroidal protrusions of increasing diameter spaced along a round bar. The bar was driven through the hole and the resulting interference was intended to cause radial metal flow to generate compressive stress when the mandrel was withdrawn. Use of this tooling was slow; however, laboratory results were very encouraging. Field performance was reportedly inconclusive, although specific details have not been made available.

Other methods have been proposed to reduce the incidence of bolt-hole cracking. The stress in the rail-web bolt-hole area could be reduced by increasing the cross-section (i.e., increasing the web thickness or reducing the bolt size). Increasing rail-web thickness, considering the required track replacement, does not appear cost effective. Reduction of hole diameter is not a practical solution because it would require cropping rail to remove existing bolt holes and, in addition, the hole diameter would have to be reduced to a degree that current joint-bar-fastening procedures and materials could not be used.

The objective of the work described in this report was to examine hole cold expansion as a means of improving the fatigue performance of rail-joint bolt holes. It was selected in place of pad coining because of its demonstrated performance in the aircraft industry and because of the improvements in the process (ref 4) that have been realized since the earlier work of reference 3. A limited amount of pad coining has been included in this program to briefly assess its potential.

---

[3]Wise, S., "Work Hardening Bolt Holes in Rail Ends", *Rail International,* pp 863–865, October 1960.

[4]Speakman, E. R., *Fatigue Life Improvement through Stress Coining Methods,* McDonnell Douglas paper 5506, June 1969.

The work reported herein has been divided into four distinct tasks:

- **Task I**—Develop a test plan to examine means of introducing compressive residual stresses into the rail web surrounding bolt holes.
- **Task II**—Examine means of introducing compressive residual stresses into bolt holes, optimize a process, and define the procedures and facilities in specification format.
- **Task III**—Demonstrate, by laboratory test on actual rail loaded to simulate in-service state of stress, the effectiveness of a process for improving the fatigue resistance of rail joints.
- **Task IV**—Establish the requirements for a field experiment to demonstrate the effectiveness of the process, and conduct such an experiment.

2. TASK—OPTIMIZATION OF RESIDUAL-STRESS-INDUCING PROCESSES

2.1 DESCRIPTION OF PROCESSES

2.1.1 GENERAL

Two residual stress-inducing processes were selected as having potential to provide significant fatigue improvement when applied to rail joints:

- Sleeve expansion (cold expansion)
- Pad coining

The major program emphasis was directed toward evaluation of the sleeve-expansion process because of the excellent aircraft service experience developed by Boeing, the U.S. Air Force, and most major aircraft producers. Pad coining was included as a backup process and to develop data to assess its potential applicability.

2.1.2 SLEEVE-EXPANSION PROCESS

The sleeve expansion process, schematically illustrated in figure 2, consisted of pushing or pulling a high-strength steel (RC_{60}) mandrel through a solid-film-lubricated stainless-steel sleeve that was placed within the hole to be treated. The mandrel and sleeve were sized to develop a controlled radial interference fit of typically 0.050 inch as the maximum diameter section of the mandrel passed through the hole. The key to the success of the process was the solid-film-lubricated inside surface of the sleeve that permitted the mandrel to be pulled through the hole without metal seizure under the estimated 500,000-psi contact stress. The sleeve was held in the hole primarily by friction between its unlubricated outside surface and the bore of the hole. Initial positioning of the sleeve was achieved by bearing one end against the nosepiece of the puller fixture. Positioning was also achieved by using a flare on the sleeve as shown by the dotted lines in figure 2. The sleeve thickness was 0.012 inch, and it was made from full-hard-type 301 stainless steel.

2.1.3 PAD-COINING PROCESS

The pad-coining process, schematically illustrated in figure 3, consisted of pressing hardened-steel circular dies against opposite surfaces of the hole to be treated and applying sufficient force to press the pads several thousandths of an inch into the surfaces.

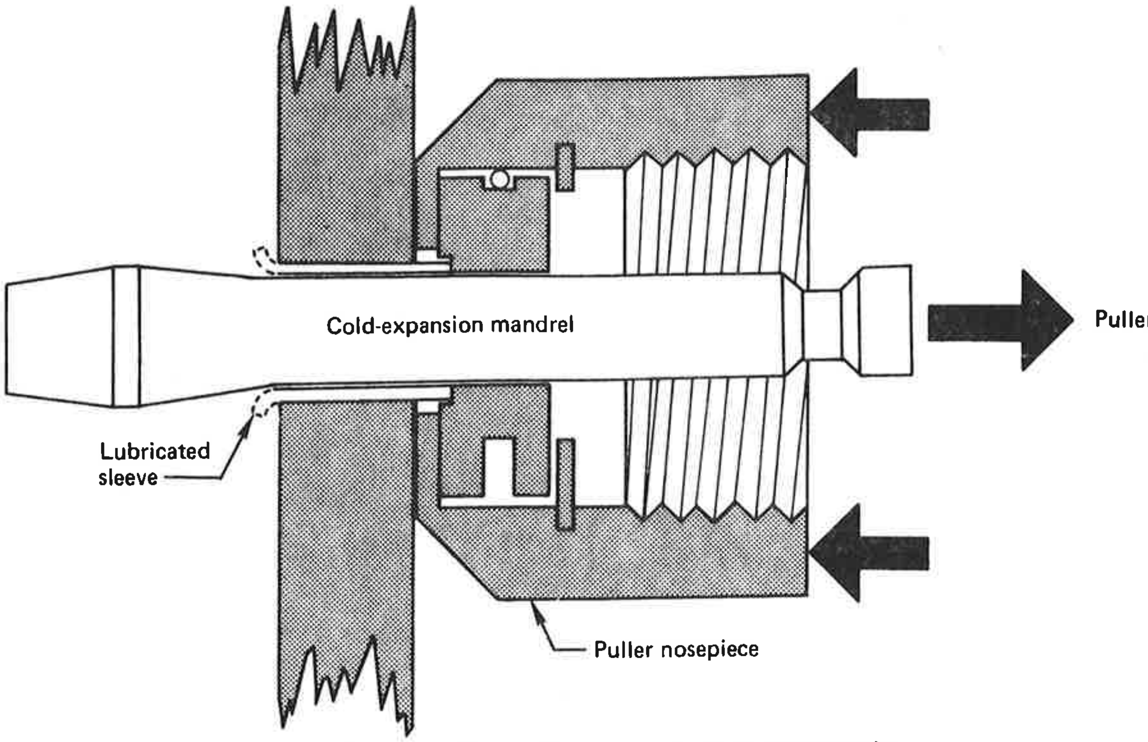

Figure 2.—Sleeve-Expansion-Process Schematic

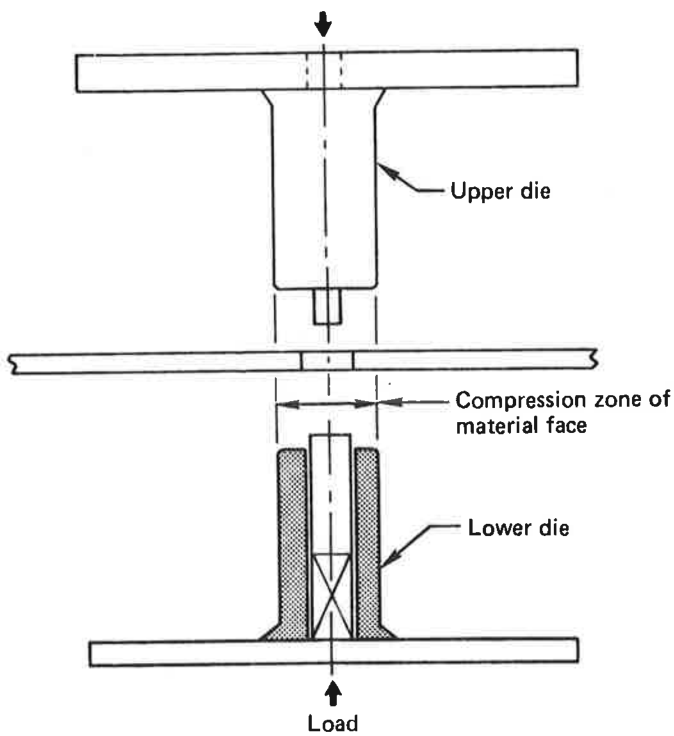

Figure 3.—Pad Coining

2.1.4 RESIDUAL STRESS

The tangential residual stress resulting from both sleeve expansion and pad coining is illustrated in figure 4. The tangential compressive stress extends from the edge of the hole, is approximately one hole radius for the hole-expansion process, and corresponds to the edge of the circular coining die for the pad-coining process. The peak value of the tangential compressive stress is greater than 80% of the yield strength of the material. A radial compressive stress also is developed. It is zero at the free edges of the part and reaches a peak value near the point where the tangential stress changes from compression to tension. This also is the approximate position of the elastic-plastic interface developed during processing.

2.2 TECHNICAL APPROACH

The technical approach to optimization of the sleeve-expansion process and evaluation of the pad-coining process was to experimentally determine the level of mandrel/hole interference or pad indentation required to achieve the greatest improvement in fatigue performance in mild steel having a pearlitic microstructure. In the case of sleeve expansion, the effect of hole diameter and hole roundness also was investigated. Figure 5 defines the variables studied. Fatigue performance was determined using an axially loaded specimen (fig. 5) to represent the type of geometry present in a rail bolt hole. The state of stress was not developed by shear loading, as in the case of a rail; however because rail failure starts at or near a point of uniaxial tension (surface of the bolt hole) the simple tensile fatigue specimen was considered a representative optimization test.

2.3 MATERIAL

AISI 1075 steel plate, 0.222-inch thick, was used to simulate rail steel. This thickness was selected because of the unavailability of more desirable 0.375- to 0.500-inch plate. Material was obtained in the annealed condition with a spheroidized annealed microstructure, necessitating normalizing to achieve a fine pearlitic microstructure. Normalizing heat treatment was accomplished by cutting plates into final specimen size, placing each specimen into a protective envelope that was evacuated to avoid decarburization, and batch processing in an air furnace. Microstructure of the heat-treated AISI 1075 steel is compared with typical rail-steel microstructure in figure 6. Composition and mechanical strength of heat-treated AISI 1075 steel plate is presented and compared with typical rail steel in tables 1 and 2, respectively.

Rail steel used for comparison was taken from 112-lb RE rail rolled during 1944–1947 and used for the laboratory rail tests reported in section 3.

2.4 EXPERIMENTAL PROCEDURE

2.4.1 SLEEVE EXPANSION

Sleeve expansion was performed as illustrated in figure 2, using a universal testing machine in place of a portable puller so that maximum loads could be determined. The test setup is shown in figure 7.

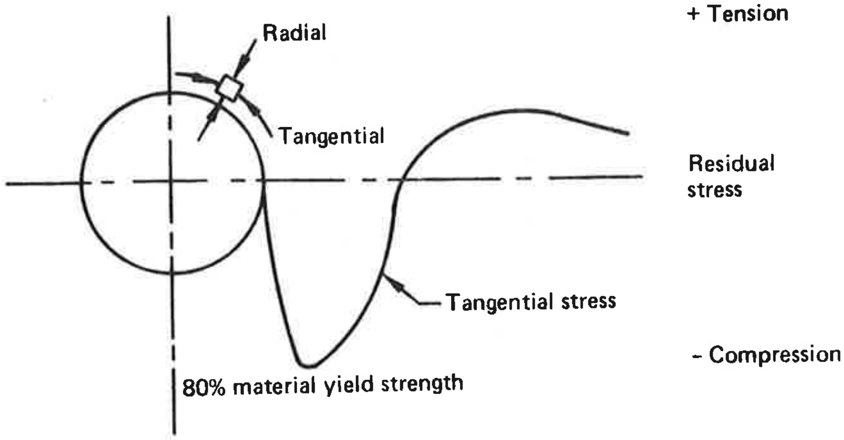

Figure 4.—Hole Compressive Stress

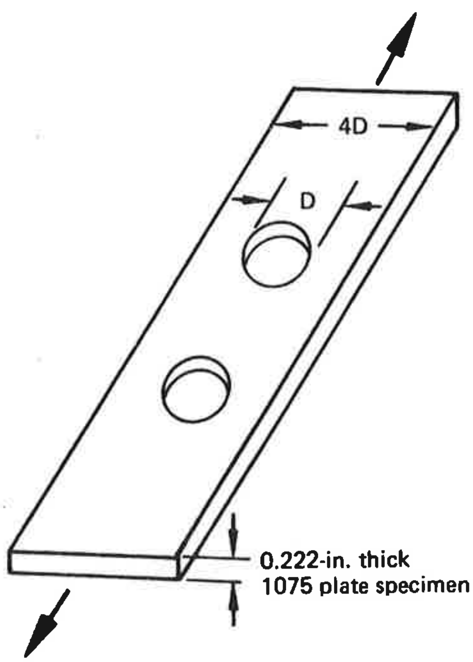

Hole treatment	Hole diameter
None Coined	1.0 1.0
None 0.025 expansion 0.043 expansion 0.053 expansion 0.064 expansion	1.25 1.25 1.25 1.25 1.25
None 0.038 expansion 0.045 expansion 0.055 expansion	1.50 1.50 1.50 1.50
0.064 expansion typical (0.050 out-of-round) [1]	1.25

[1] Elongated axis inclined 45° to specimen axis.

Figure 5.—Process-Optimization Details

A. 1075 PLATE PEARLITIC MICROSTRUCTURE (500X)

B. 112-LB RAIL MICROSTRUCTURE (500X)

Figure 6.—Microstructure

Table 1.—1075-Plate Chemical Composition Compared with Rail Chemical Composition

Sample		Element									
		C [1]	Mn	Si	Ni	Mo	Cr	Cu	V	P	S
1075 plate		0.78	0.51	0.19	0.006	0.01	0.10	0.01	0.003	0.021	0.012
AREA specification for 91/120-lb rail, revised 1970		0.67/ 0.80	0.70/ 1.00	0.10/ 0.25	— —	— —	— —	— —	— —	0.04 —	0.05 —
Program rail samples											
No.	Serial no.										
1	CC22358B	0.81	0.82	0.20	0.038	0.01	0.11	0.016	0.01	—	—
2	CC32675F	0.77	0.80	0.16	0.035	0.01	0.10	0.03	0.01	—	—
3	CC10375C	0.81	0.90	0.18	0.032	0.01	0.10	0.01	0.01	—	—
4	CC88031E	0.74	0.82	0.14	0.041	0.01	0.11	0.028	0.01	—	—
5	CC470564F	0.81	0.78	0.16	0.031	0.01	0.10	0.014	0.01	—	—
6	CC790515E	0.82	0.80	0.16	0.036	0.01	0.10	0.027	0.01	—	—

[1] Measured value ±0.03.

Table 2.—Comparison of Mechanical Properties of 1075 Plate and Rail Steel

Specimen no.	Normalized 1075 steel UTS (ksi)	Normalized 1075 steel YTS (ksi)	Normalized 1075 steel e (%)	Rail no.	112 lb/yd rail steel UTS (ksi)	112 lb/yd rail steel YTS (ksi)	112 lb/yd rail steel e (%)
1	134	69.7	17.0	1	139.9	75.3	15.0
2	123.3	64.6	17.5	3	140.9	76.8	12.0
3	131.6	65.7	18.5				
4	133.2	68.4	16.5				
5	134.5	70.0	16.0				
6	134.3	69.7	16.0				

Notes:
- See Table 1 for extremes of rails 1 through 6.
- UTS—ultimate tensile strength
- YTS—yield tensile strength
- e—elongation

2.4.2 PAD COINING

Pad coining was accomplished as illustrated in figure 3, using a universal test machine to apply the load and measure the peak load. The test setup is shown in figure 8. The test specimens were loaded until a pad indentation of 0.002 to 0.005 inch was measured, and the maximum load was recorded.

2.4.3 FATIGUE TEST

Fatigue tests were conducted in a 100-kip Vibraphore hydraulic fatigue machine operating at 4000 cycles/minute. The test setup is shown in figure 9. Tests were conducted in an ambient environment at R = 0.06 (R = minimum stress/maximum stress), over a range of stress levels under constant-amplitude conditions. A segment of an S-N (stress level versus number of cycles to failure) curve was developed.

The 0.222-inch-thick plate proved to be too thin to stabilize the high compressive stresses developed by cold expansion, resulting in a local buckling (oil canning) around the hole. This does not occur in the much thicker and stiffer rail sections. To evaluate the effect of plate buckling on fatigue performance, 0.75-inch-thick plates with low-friction interface shims were bolted on both sides of the test specimens, using bolts through, but not touching, the holes and then fatigue tested. An identical test for a non-expanded specimen demonstrated that the procedure would not, in itself, improve fatigue life.

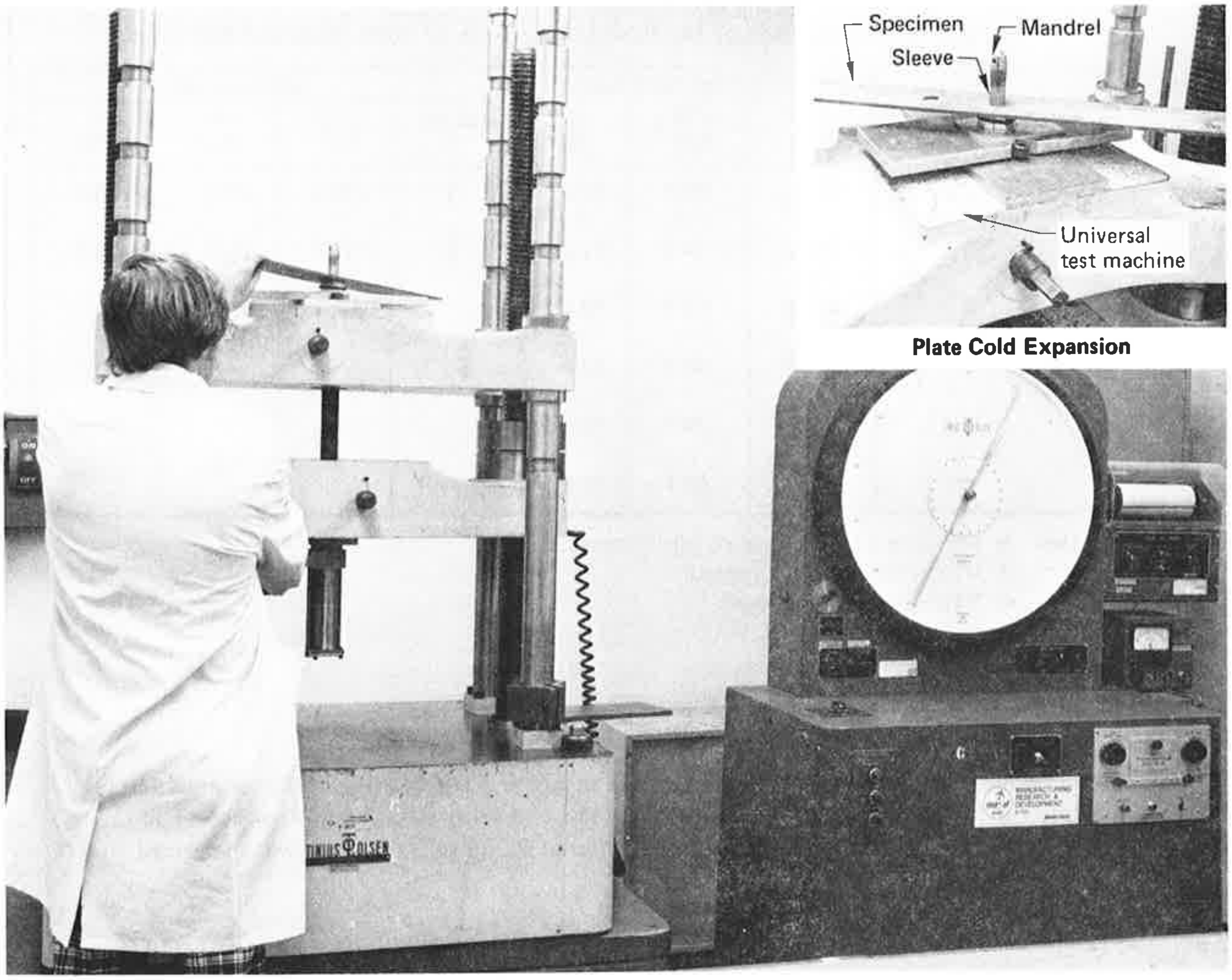

Plate Cold Expansion

Sleeve Cold Expansion

Figure 7.—Sleeve and Plate Expansion in Universal Test Machine

2.5 TEST RESULTS

2.5.1 SLEEVE-EXPANSION AND PAD-COINING LOADS

Loads required for sleeve expansion of different hole sizes are presented in figure 10 for different hole sizes. The load required for coining depended on the size of pad used. The surface-bearing stress required was 70,000 psi.

2.5.2 FATIGUE TESTS

Fatigue test data are tabulated in appendix A and graphically presented in figures 11, 12, and 13.

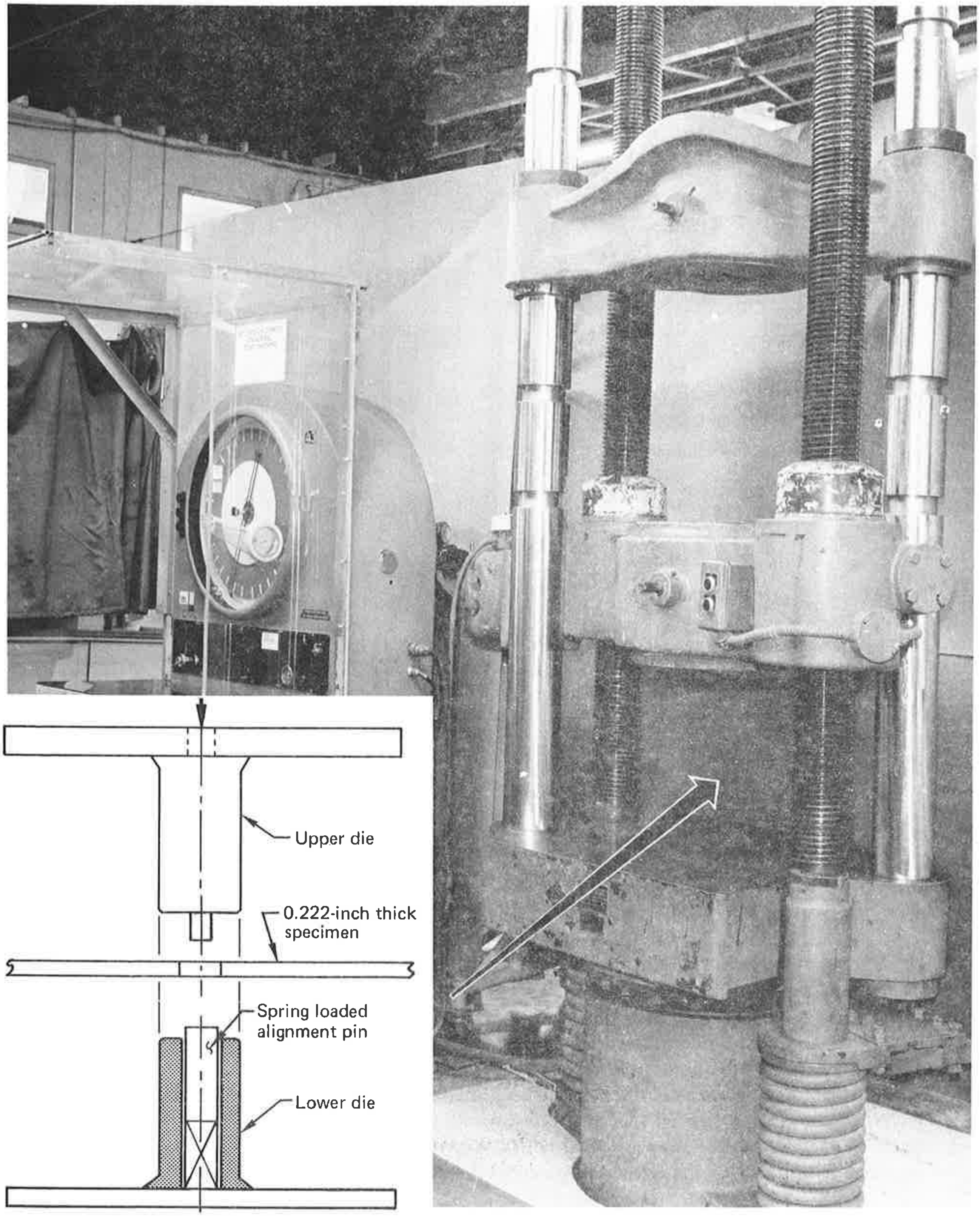

Figure 8.—Pad Coining in Universal Test Machine

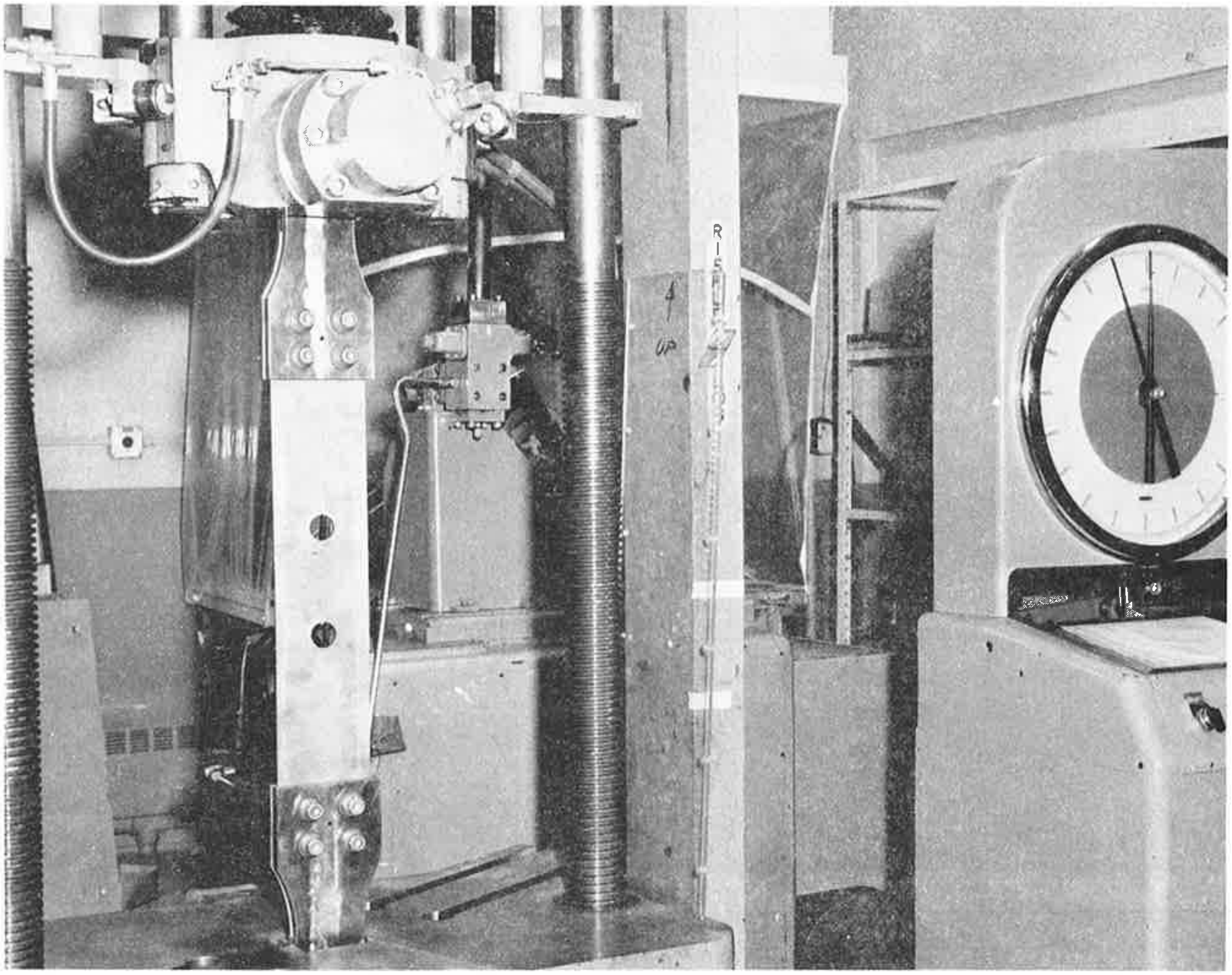

Figure 9.—1075-Plate Fatigue Test

2.6 DISCUSSION OF RESULTS AND CONCLUSIONS

It is clearly evident that the thinness of the AISI 1075 steel plate had a detrimental impact on the hole-expanded specimens. A review of figure 11 indicates that the 1.25- and 1.50-inch-diameter-hole specimens, tested without correction for specimen distortion, show an increase in fatigue-life properties when compared to the baseline (noncold expanded) 1.25- and 1.50-inch-diameter-hole specimens. However, the hole-expanded specimens tested without correction did not demonstrate the fatigue-life improvement of the 1.25-inch-diameter-hole expanded specimens tested with correction for plate buckling, clamping (sec. 2.4.3), and the coined specimens. This last group, figure 12, demonstrated a significant improvement in fatigue life when compared to the non-cold-expanded specimens.

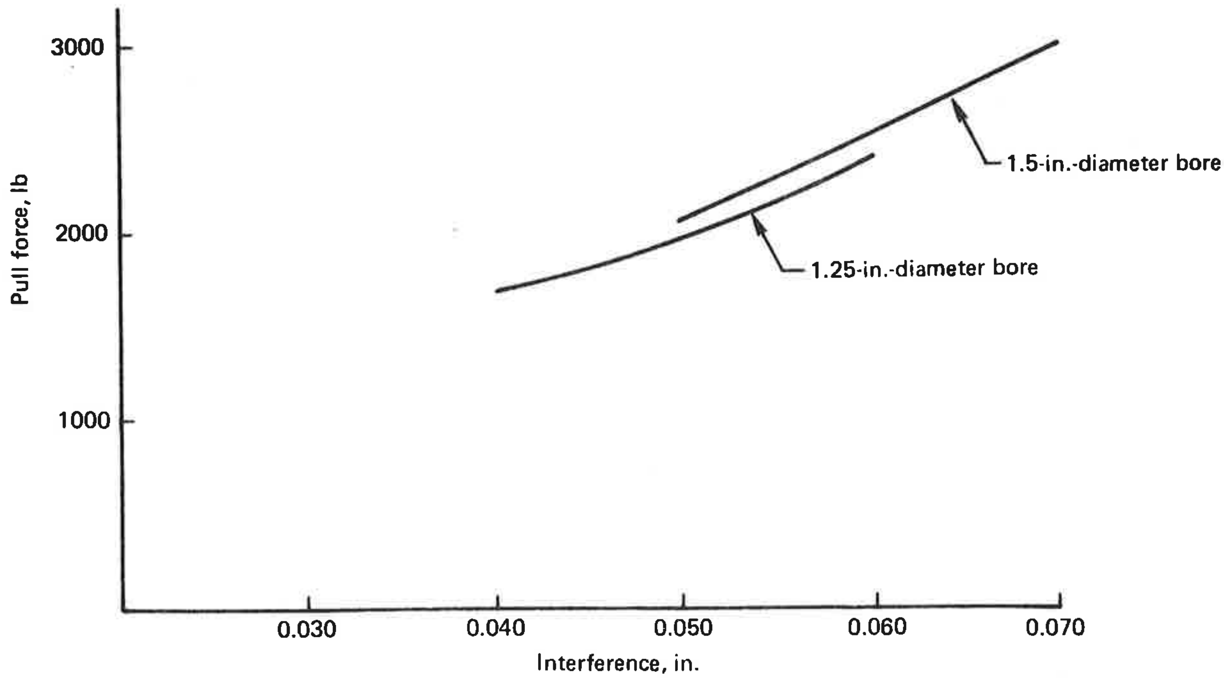

Figure 10.—Mandrel Pull Force

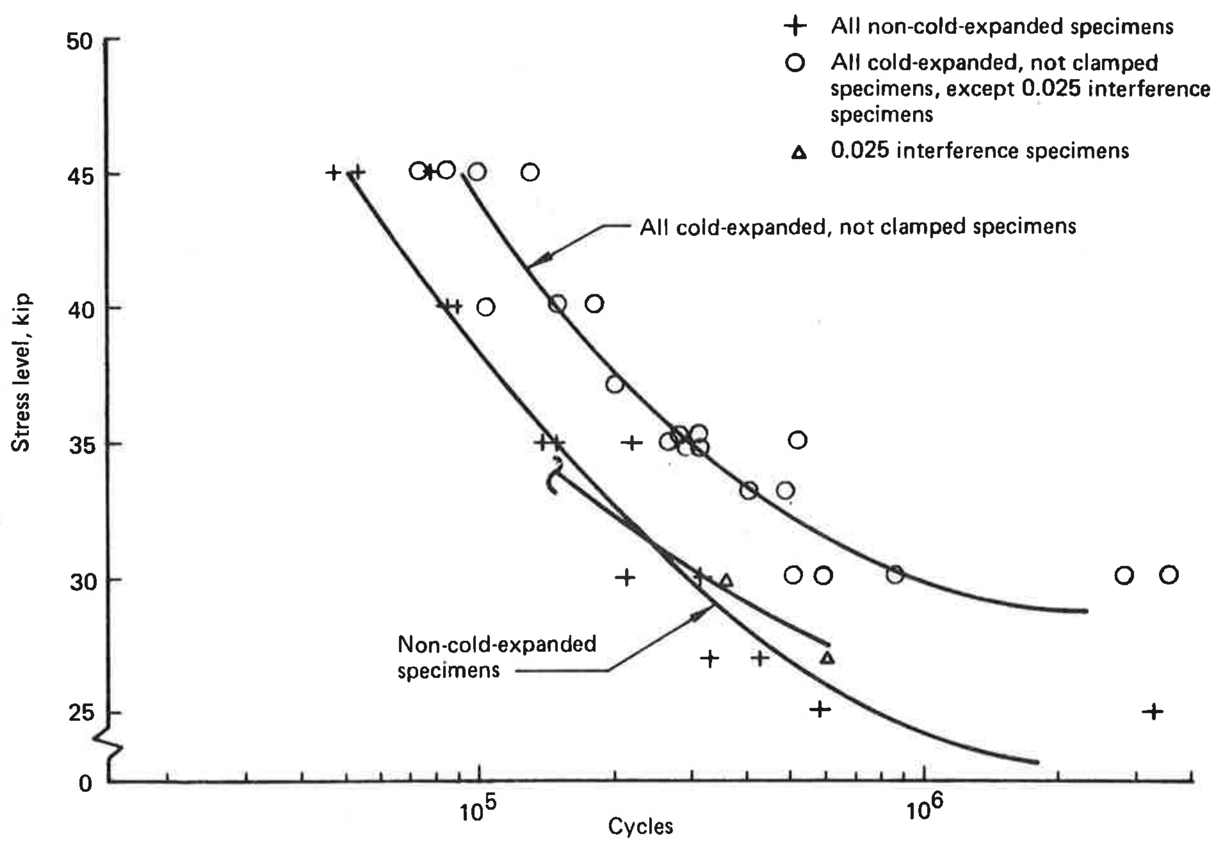

Figure 11.—Non-Cold-Expanded/Cold-Expanded, Not Clamped Specimens

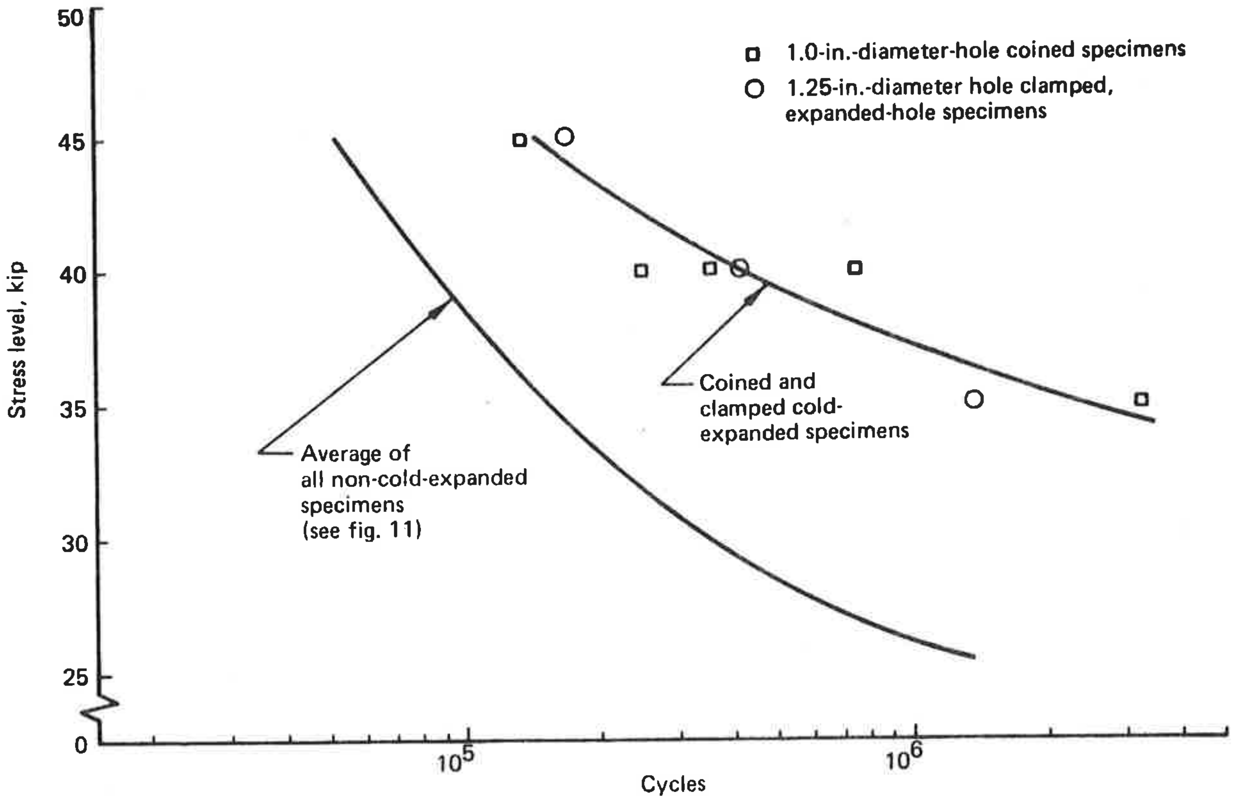

Figure 12.—Non-Cold-Expanded/Cold-Expanded, Coined, and Clamped Specimens

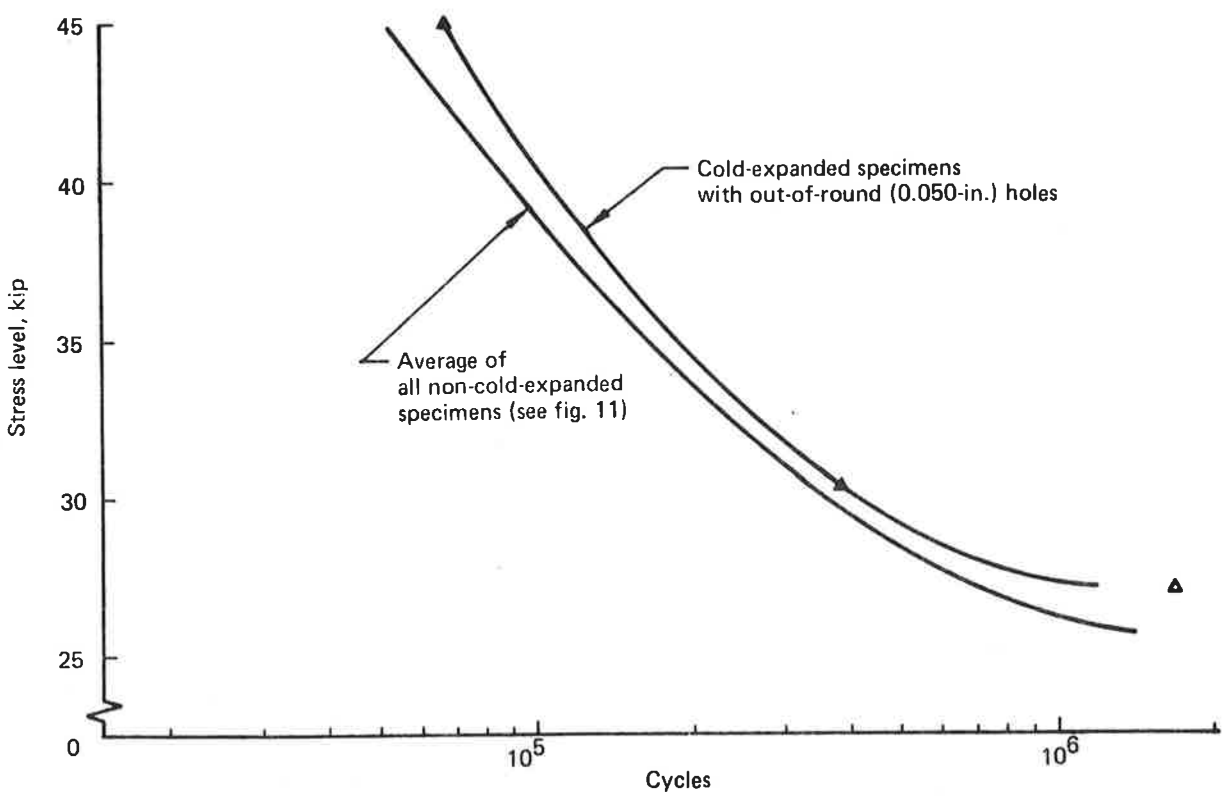

Figure 13.—Non-Cold-Expanded/Cold-Expanded, Out-of-Round-Hole Specimens

Based on these results, it was concluded that both pad coining and hole expansion would appreciably improve the fatigue-life performance of high-carbon normalized steel.

The results of the pad-coining tests indicated that coining forces in excess of 100,000 pounds (providing a face indentation of 0.004 to 0.005 inch) were required for the 0.222-inch-thick steel plate. It was calculated that a higher force would be needed for 0.60-inch-minimum rail webs, requiring a tooling development program beyond the scope of this program. In addition, data pertaining to rail-web face condition at the bolt hole, critical to pad coining, were of limited availability, placing an additional handicap on coining-process development.

The results of the hole-expansion tests show that the process is, from a fatigue-life-improvement standpoint, comparable with pad coining where correction for buckling of the thin plate specimens was made. As plate thickness increases, effectiveness of the hole-expansion process increases (ref 5). Thus, it was anticipated that the hole-expansion process would provide a fatigue-life improvement exceeding that of coining when applied to the heavier section material found in railroad rail.

The expansion tests show that an expansion of the hole, must approach 3.5% diametrical strain (an interference of 0.043 inch for 1.25-inch-diameter holes). At 5% diametrical strain (0.053-inch interference for 1.25-inch-diameter holes), no loss of mechanical properties of the plate was evident. Very low strain (interference of 0.025 inch) indicated no fatigue improvement. Therefore, the starting-hole-size relationship to mandrel size shown in table 3 was developed to provide the interference, and subsequent diametrical strain, planned for the tests on actual rail conducted under Task IV (sec. 4.0).

Table 3.—Mandrel Sizes

Starting hole diameter (in.)	Maximum mandrel diameter [1] (in. $\pm$0.0002)
1.000	1.026
1.062	1.090
1.125	1.156
1.188	1.221
1.250	1.286
1.313	1.351
1.375	1.416
1.438	1.481
1.500	1.546

[1] Mandrel is based on 0.012-in.-sleeve thickness.

---

[5]Phillips, J. L., *Sleeve Coldworking Fastener Holes,* AFML-TR-74-10, Air Force Materials Laboratory, February 1974.

The results of the tests conducted with plate specimens whose 1.25-inch-diameter holes were altered to provide a 0.050-inch out-of-round condition (fig. 13) indicated no improvement in fatigue life, demonstrating the need for starting holes within the tolerance noted in table 4. Out-of-round-hole conditions were not affected by "oil canning" because the interference that developed was not sufficient to produce the "oil-can" condition.

Table 4.—Starting-Hole Dimensions

Minimum diameter (in.)	Maximum diameter (in.)
1.000	1.010
1.062	1.072
1.125	1.135
1.188	1.198
1.250	1.260
1.313	1.323
1.375	1.385
1.438	1.448
1.500	1.510

3. TASK III–EXPERIMENT TO EVALUATE THE EFFECT OF OPTIMIZED SLEEVE-EXPANDED BOLT HOLES ON FATIGUE LIFE OF 112-POUND RE RAIL

3.1 GENERAL

The objective of this experiment was to demonstrate, by laboratory tests, comparative improvement in fatigue life achievable by sleeve expansion of bolt holes in full-size rail. The experiment was designed to include the effect of mechanical conditions encountered in service (table 5); however, no attempt was made to duplicate loading spectra or field environmental conditions.

3.2 TECHNICAL APPROACH

3.2.1 TEST PLAN

The test matrix presented in table 6 was designed to evaluate improvement in performance resulting from sleeve expansion, as well as the effect of commonly encountered conditions of fretting, hole elongation, geometry, and undetected cracks. The original test matrix was designed as a balanced and complete block to permit statistical analysis of data. An additional test for cold expansion on rails with preexisting cracks was added after the test was in progress. Rails from the nonfretted, non-cold-expanded test were reused, and only the precracked portion was unbalanced. The experimental-design randomly selected specimens from the six different rails used as source material and evaluated the conditions of fretting, hole elongation, geometry, and small undetected cracks. Data acquisition was designed to permit use of extreme-value techniques, necessary to plan the field experiment discussed in section 4.

3.2.2 RAIL SELECTION AND PROPERTIES

The rail section selected for test was 112-lb/yd RE, based on the fact that it is a very common rail section used in the United States for mainline service. In addition, rails of this type have exhibited sufficient history of bolt-hole failure (sec. 4.1) to warrant attention of the test program.

The metallurgical structure, chemical composition, and mechanical properties of test rails are presented in section 2.3. Rails previously used in service were selected for the experiment to duplicate, to a degree, surface corrosion and pitting conditions.

Table 5.—Mechanical Conditions Studied

No.	Mechanical condition	Description	Test condition
1	Fretting	Joint-bar bolt loaded on bolt-hole bore by rail tension.	Bolt in contact with hole bore.
2	Hole elongation	Hole deformation created by bolt shear/rail tension.	Hole elongated under static conditions by bolt bearing. Bolt not in contact with hole bore during fatigue test.
3	Hole spacing		Hole spacing examined by testing two- and four-hole specimens.
4	Small cracks		Fatigue testing of specimens containing a crack approximately 1/8 in. long, initiating from bolt holes.

Table 6.—Test Matrix

<table>
<tr><th colspan="3" rowspan="2">Type</th><th colspan="2">Condition</th></tr>
<tr><th>Non-cold-expanded</th><th>Cold-expanded</th></tr>
<tr><td rowspan="8">Original test matrix</td><td rowspan="2">Nonfretted</td><td>A</td><td>8</td><td>8</td></tr>
<tr><td>B</td><td>1 1 2 2 5 5 6 6</td><td>1 1 2 2 5 5 6 6</td></tr>
<tr><td rowspan="2">Fretted</td><td>A</td><td>8</td><td>8</td></tr>
<tr><td>B</td><td>1 1 2 2 5 5 6 6</td><td>1 1 2 2 5 5 6 6</td></tr>
<tr><td rowspan="2">Four holes</td><td>A</td><td>4</td><td>4</td></tr>
<tr><td>B</td><td>5 5 6 6</td><td>5 5 6 6</td></tr>
<tr><td rowspan="2">Elongated</td><td>A</td><td>4</td><td>4</td></tr>
<tr><td>B</td><td>1 1 2 2</td><td>1 1 2 2</td></tr>
<tr><td rowspan="2">Additional tests</td><td rowspan="2">Precracked [1]</td><td>A</td><td>3</td><td>3</td></tr>
<tr><td>B</td><td>1 2 2</td><td>5 6 6</td></tr>
</table>

A—Number of rail specimens tested

B—Rail numbers where specimens were taken (see table 1)

[1] Rails reused from nonfretted, non-cold-expanded tests.

3.3 EXPERIMENTAL PROCEDURE

3.3.1 TEST-SPECIMEN DESIGN AND STATE OF STRESS

Design of the rail specimen was predicated on producing a nearly pure shear loading of the rail web in the area of the bolt holes. The 24-inch-long specimens were prepared to the designs shown in figure 14, providing for both two-hole and four-hole configurations. Use of two specimen configurations provided the variables of number of holes and hole spacing. Specimen length and hole pattern were established to generate desired web stress when the specimen was loaded as a simple beam with a 5-inch-long distributed load symmetrical about centerline (fig. 15). Thus, web shear loads were calculated to be:

$$\tau = 29.2 \text{ ksi}$$

$$\sigma_{max} = \pm 29.2 \text{ ksi}$$

at 170-kip loading of the central 5-inch-long area.

Prior to fatigue testing, the state of stress of the two- and four-hole rail specimens, when loaded at 170 kips, was experimentally determined. A specimen of each configuration was instrumented with strain gages as shown in figure 16. The specimen then was placed in the fatigue test fixture and loaded statically. An additional loading device, a turnbuckle arrangement (fretting fixture), described in section 3.3.3.1 and illustrated in figure 15, was used as a compression member to apply a load between the bolt holes of the two-hole specimen. When loaded, strain at points on the specimen (indicated in figure 17) was recorded by strain readout instrumentation. These data were processed by computer program to establish the specimen state of stress.

3.3.2 SPECIMEN PREPARATION

3.3.2.1 Drilling and Sleeve Expansion

The 112-lb/yd rails were cropped and drilled to the design shown in figure 14. Drilling of the bolt holes was accomplished with a flat, spade-type drill, the type normally used for track-drilling operations. No additional hole treatment to improve the surface bore of the drilled holes (e.g., reaming, broaching, or deburring) was used. All specimens were identified by the code marking shown in table 7.

In-service rail has 1-1/8-inch-diameter bolt holes. To cold expand the holes for the field-service tests (Task IV, section 4.0), it was necessary to clean the holes prior to cold expansion and to produce finished holes of the standard sizes used for track application. Therefore, the specimen holes to be cold expanded were drilled to 1.1875-inch diameter. The remaining (non-cold-expanded) specimens were drilled to 1.25-inch diameter. The specimens with 1.1875-inch-diameter holes then were cold expanded, bringing the diameter to 1.245 inches, less the 0.008- to 0.010-inch-diameter springback of the hole size that normally occurs when the mandrel is removed from the hole.

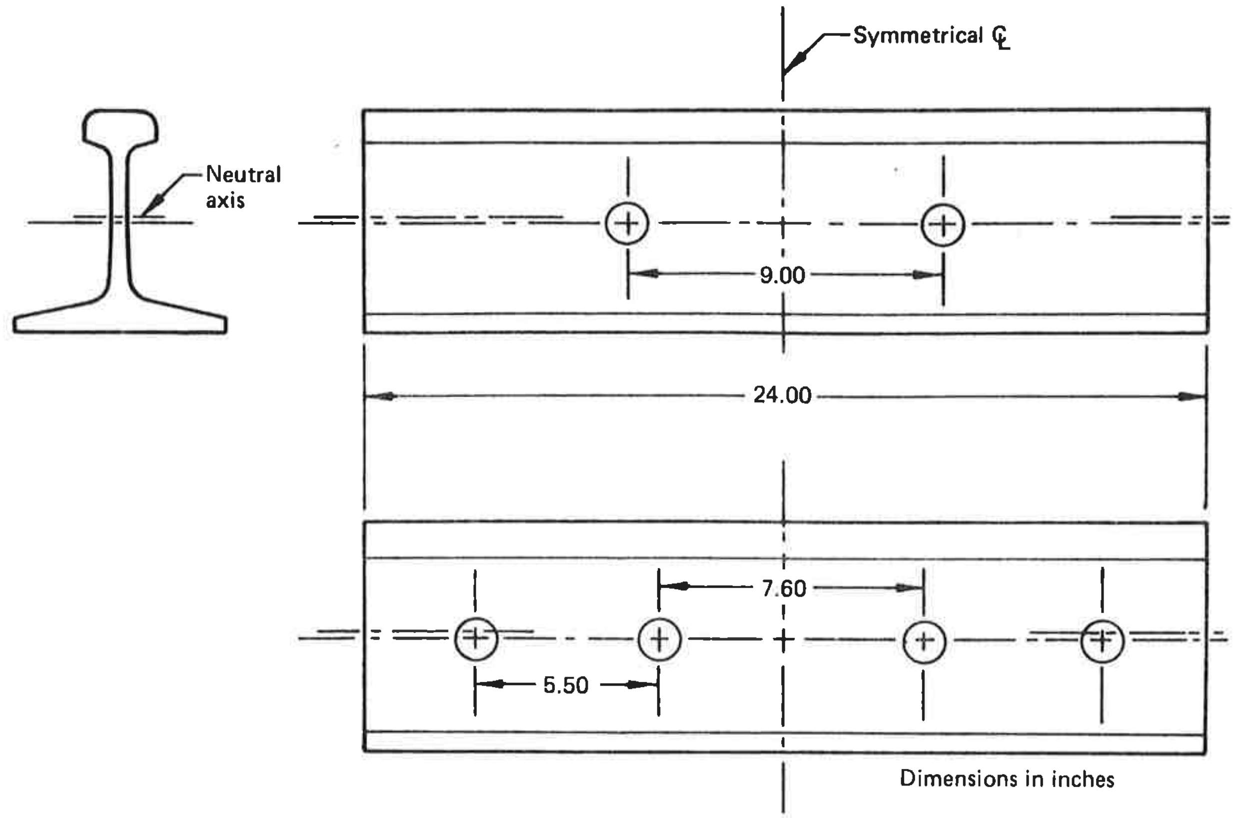

Figure 14.—Specimen Design

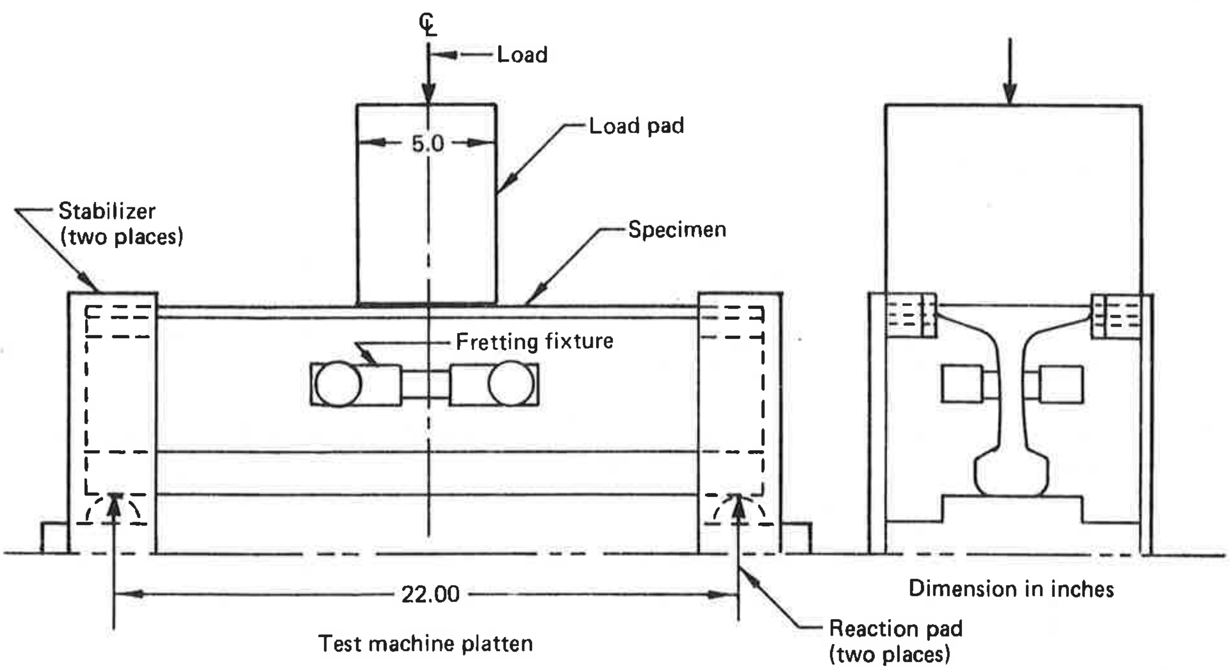

Figure 15.—Fatigue Test Fixture

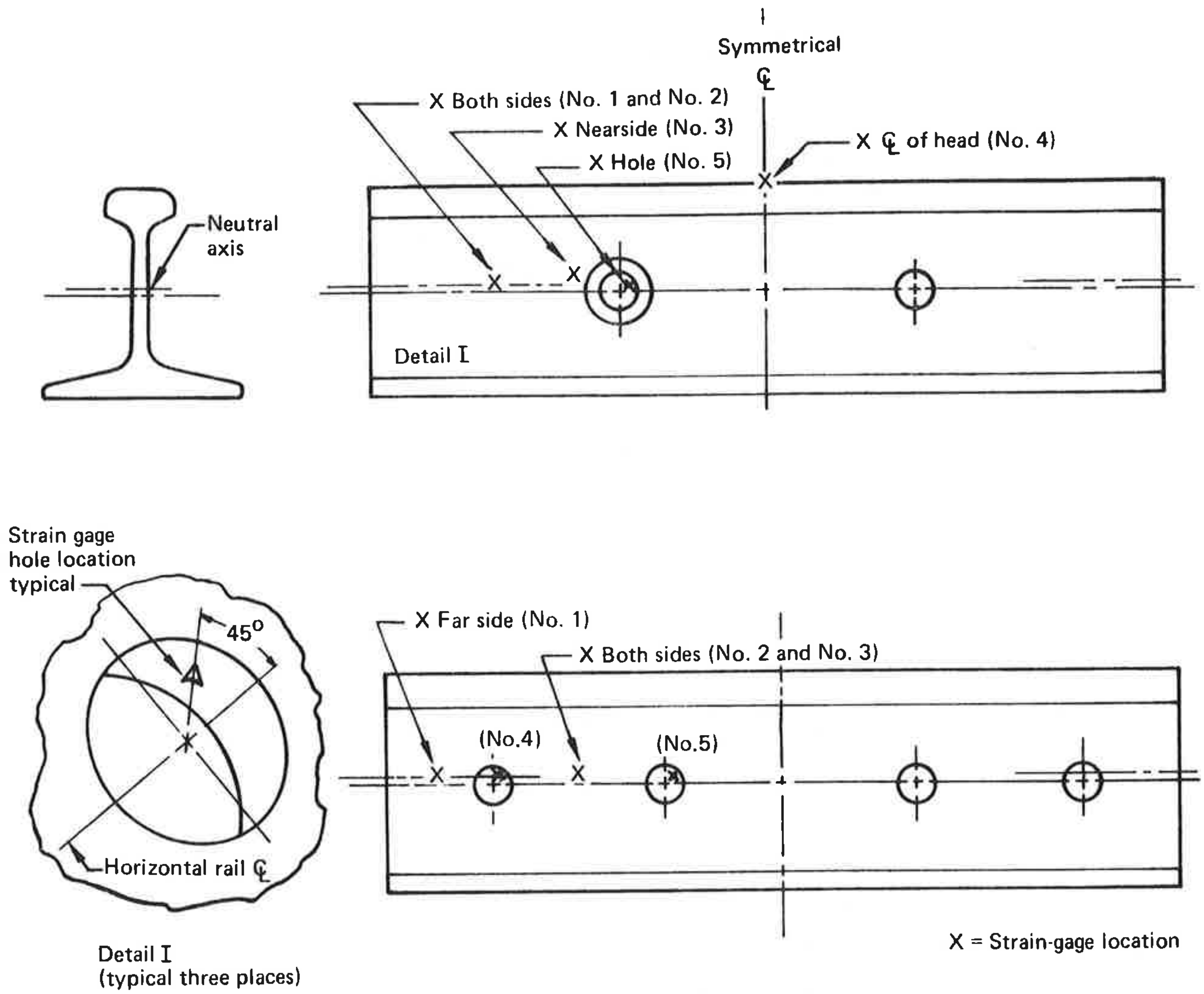

Figure 16.—Strain-Gage Location

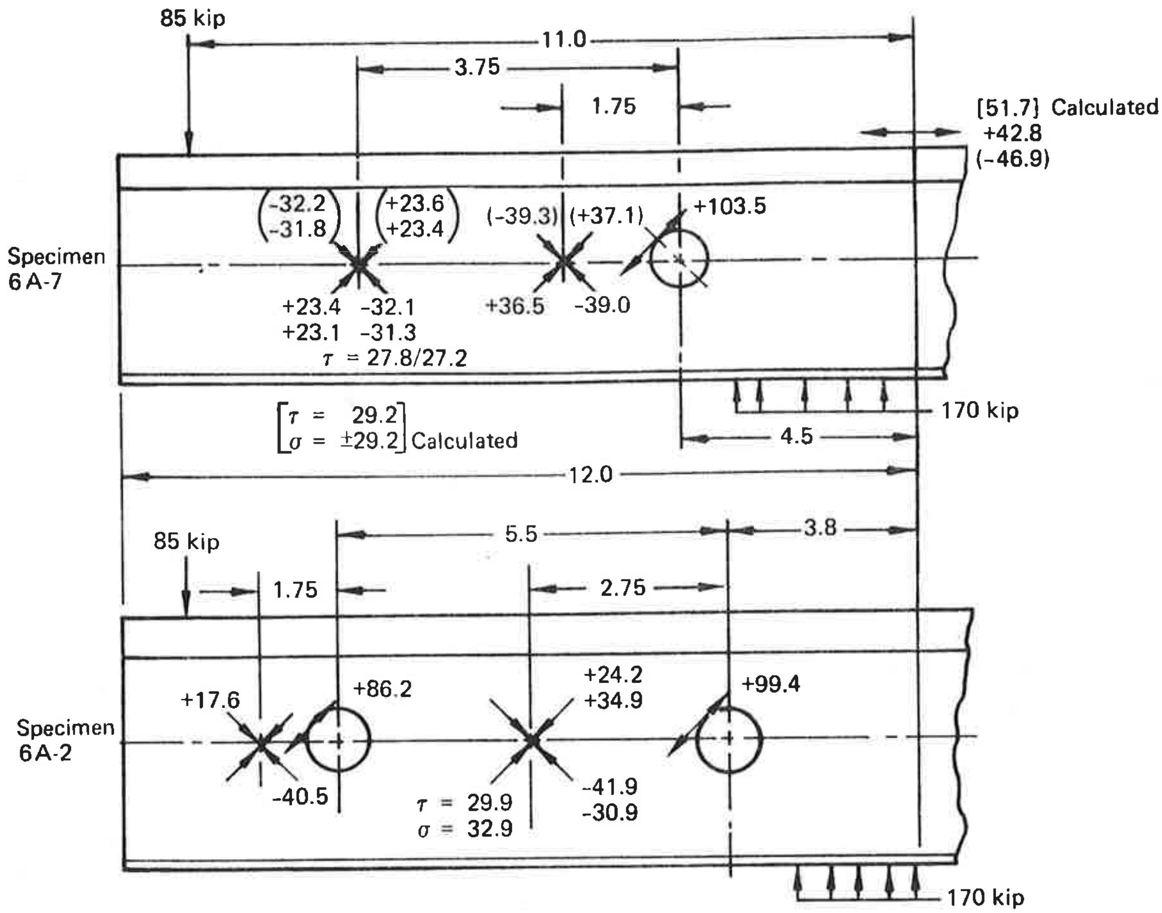

Notes:
- Dimensions in inches, stress measurements in ksi, all others as noted.
- Measurements in parenthesis measured with fretting fixture attached and loaded. Hole diameter = 1.25 in.
- Where two data are given, two back-to-back gages were used.

Figure 17.—Rail Stress

Table 7.—Specimen Identification Code

Code no.	Hole treatment	Hole pattern	Rail no.
1A-1 through -8	Non-cold expanded	Two hole	1
1B-1 through -8	Cold expanded		1
2A-1 through -8	Non-cold expanded		2
2B-1 through -8	Cold expanded		2
3C-1 through -7	Non-cold expanded		3
3D-1 through -7	Cold expanded		3
5A-1, -2, -6, -7, -8	Non-cold expanded		5
5B-1, -2, -6, -7, -8	Cold expanded		5
6A-1, -4, -5, -7	Non-cold expanded		6
6B-1, -2, -6, -7, -8	Cold expanded	Two hole	6
5A-3, -4, -5	Non-cold expanded	Four hole	5
5B-3, -4, -5	Cold expanded		5
6A-2, -3, -6	Non-cold expanded		6
6B-3, -4, -5	Cold expanded	Four hole	6

Note: Specimens 5A-2, 6A-1, and 6A-4 were cold expanded for precrack test after initial crack evidence.

Cold expansion of the rail specimens was accomplished with a portable mandrel pull gun and air-operated hydraulic power supply capable of exerting 18,000-pound pull force. The cold expansion process, mandrel, and lubricated sleeve used for cold expansion of the rail specimens were as described in section 2, except for the use of the portable pull gun (figs. 18 and 19.).

Some difficulty was experienced in sleeve expanding the first rail specimens, as mandrel pull forces approached 16,000 pounds. This problem was caused by inadequate lubricant (dry film) coating on the sleeve interior. The sleeves were returned to the supplier and relubricated. This problem primarily was a result of the large-diameter sleeves, exceeding the diameter of those normally produced, creating a conflict with normal lubricant coating and quality-control procedures. The supplier's procedures were altered to compensate for the larger sleeve diameters, and correctly lubricated sleeves were supplied. As a result of sleeve lubricant correction, pull forces required to cold expand the remaining rail specimens were reduced to 8,000 pounds maximum.

The rail from which the specimens were taken exhibited a heavy oxide coating on the web surfaces. During the cold-expansion process, the coating was displaced by web plastic flow induced by the cold-expansion process. The result was a visible pattern on the rail web defining the compressive-stress area, figure 20. The area of displaced oxide coating closely approximated the area of the web calculated to be affected by the cold-expansion process, figure 4.

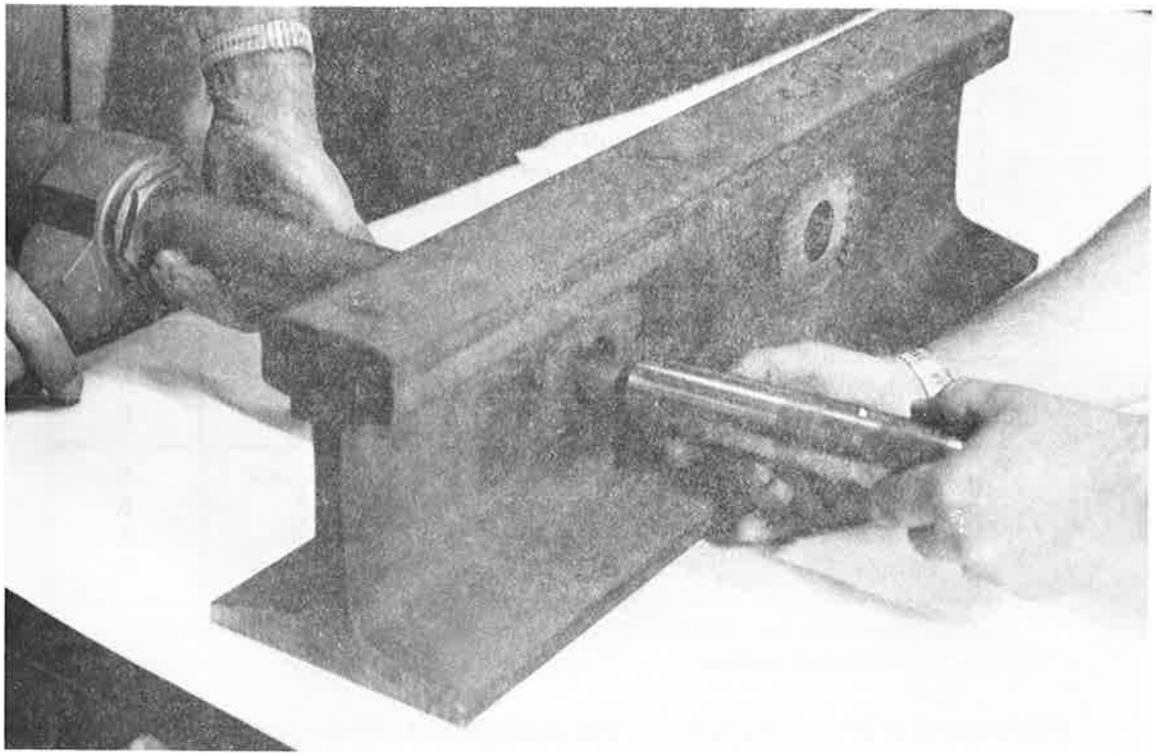

Figure 18.—Mandrel and Pull-Gun Application

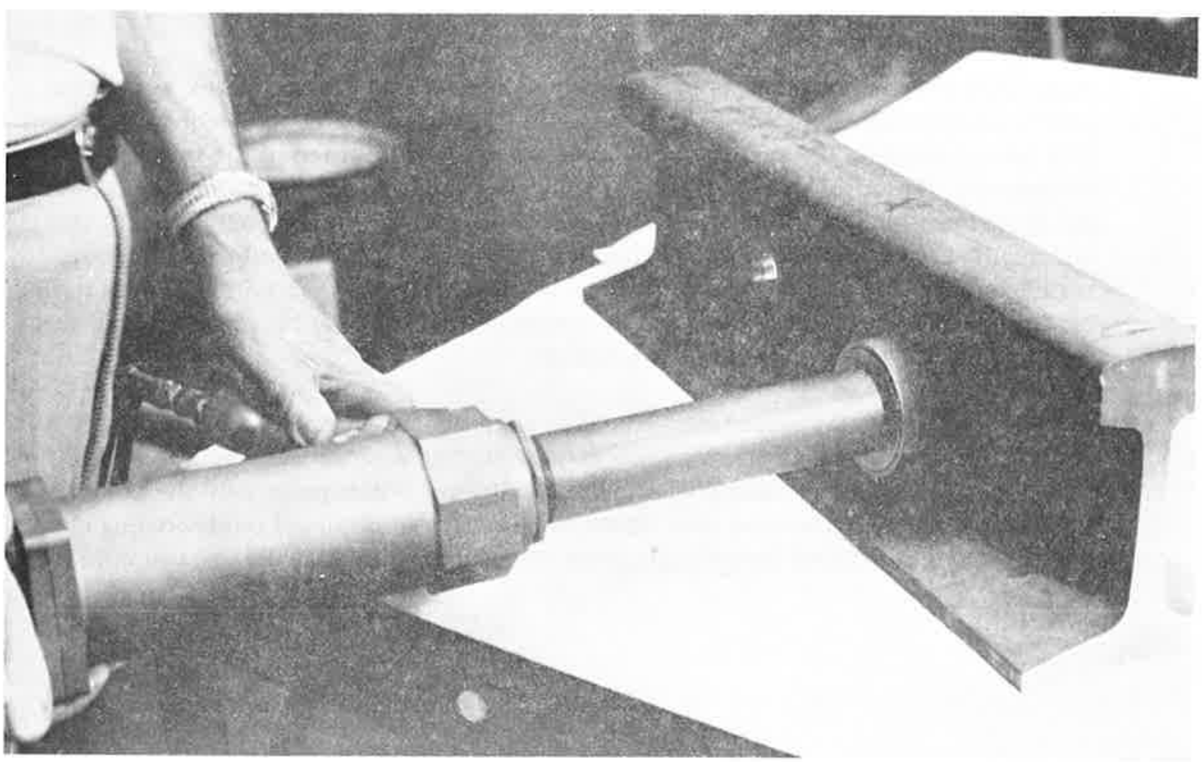

Figure 19.—Cold-Expansion Pull Gun

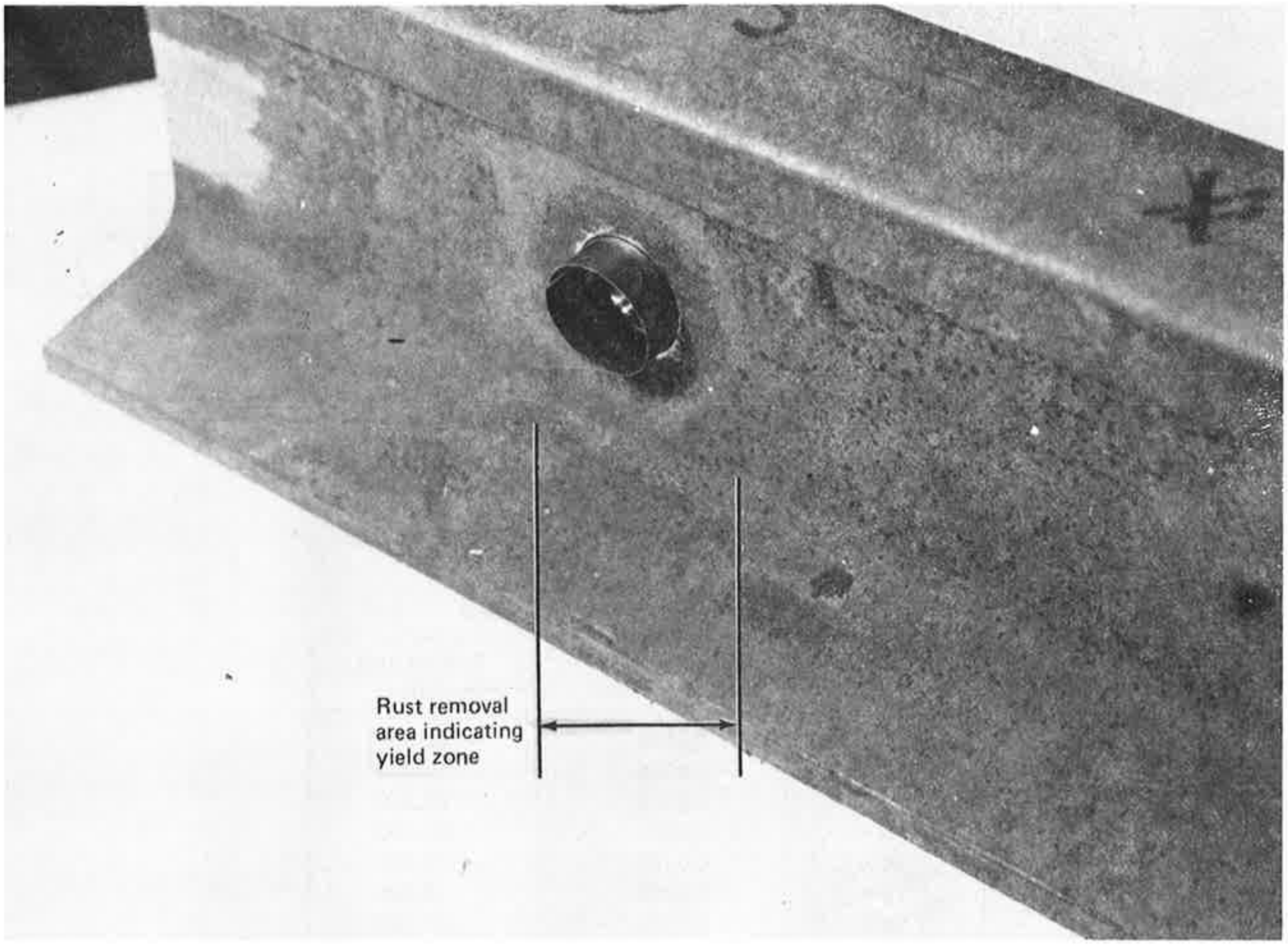

Figure 20.—Strain Pattern Visible in Rusted Rail

3.3.2.2 Hole Elongation Representing Rail Thermally Induced Tension

The load-induced elongated holes in both non-cold-expanded and cold-expanded specimens were developed by pin loading the specimen, using a 1-inch-diameter pin as illustrated in figure 21. A load was applied until a deformation was detected. Deformation and loads are shown in table 8.

3.3.2.3 Preexisting Fatigue Cracks Representing Undetected Service Cracks

Six non-cold-expanded specimens from the nonfretted tests that exhibited cracks approximately 0.25-inch long were selected. The 1.25-inch-diameter holes of three specimens were reamed to 1.5-inch diameter, leaving an approximately 0.125-inch-long crack remaining. The holes of the three other specimens were reamed to 1.4375 inches in diameter and cold expanded to a diameter of 1.480/1.490 inches, leaving a 0.1875-inch-long crack. Crack detection circuit wires (sec. 3.3.3.2) were placed 0.70 inch from the edge of the holes.

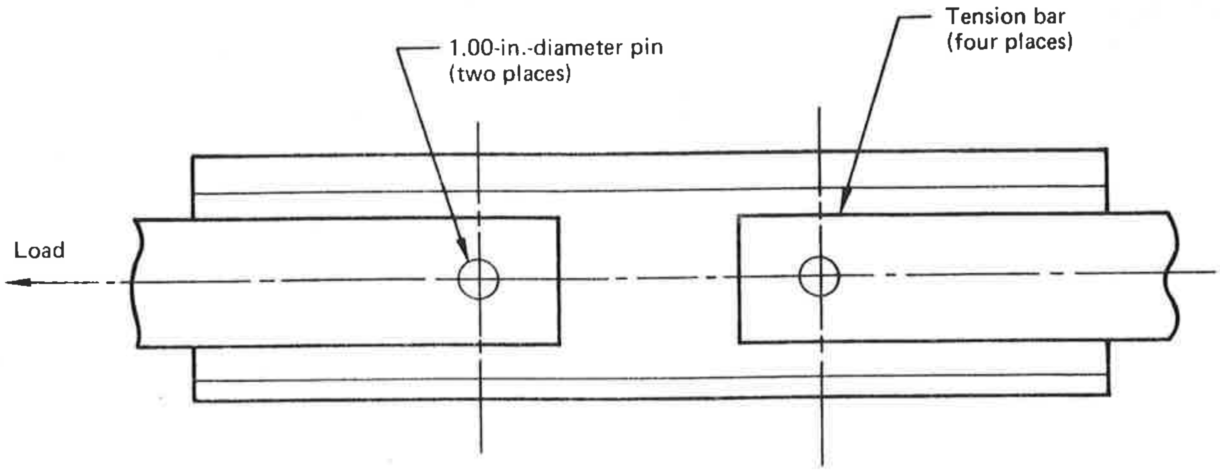

Figure 21.—Elongation Fixture

Table 8.—Hole-Elongation Data

Specimen no.	Deformation—major axis (in.)	Tension load (lb)
1A-5	0.0866	150,000
1A-6	0.0065	50,000
2A-5	0.0069	50,000
2A-6	0.0071	50,000
1B-5	0.0122	75,000
1B-6	0.0082	75,000
2B-5	0.0182	100,000
2B-6	0.0109	75,000

3.3.3 FATIGUE TEST SETUP AND PROCEDURE

3.3.3.1 Test Machine and Setup

The fatigue tests were performed using a 180-kip double-acting fatigue machine operating at 10 Hz. The rail specimens were mounted in the inverted position, the rail head supported at 22-inch centers, with the machine load pad driving downward on the rail base (figure 15). A 5- by 5- by 8-inch pad applied load forces to produce a fatigue ratio of 0.05. Figure 22 shows the actual specimen loaded in the test machine. The pad initially was made of oak; however, the low modulus of oak resulted in the rail base bending and cracking (fig. 23) at the large number of cycles required to fail the sleeve-expanded specimens. The block was changed to aluminum and rail base cracking was no longer observed.

The test setup was altered for the fretting tests. A double turnbuckle arrangement was attached to 1.0-inch-diameter pins in each hole (fig. 15) and a load of 8,000 pounds applied, the turnbuckles serving as compression members. Fretting motion was induced by the flexure of the specimen under the cyclic fatigue loading of the rail base.

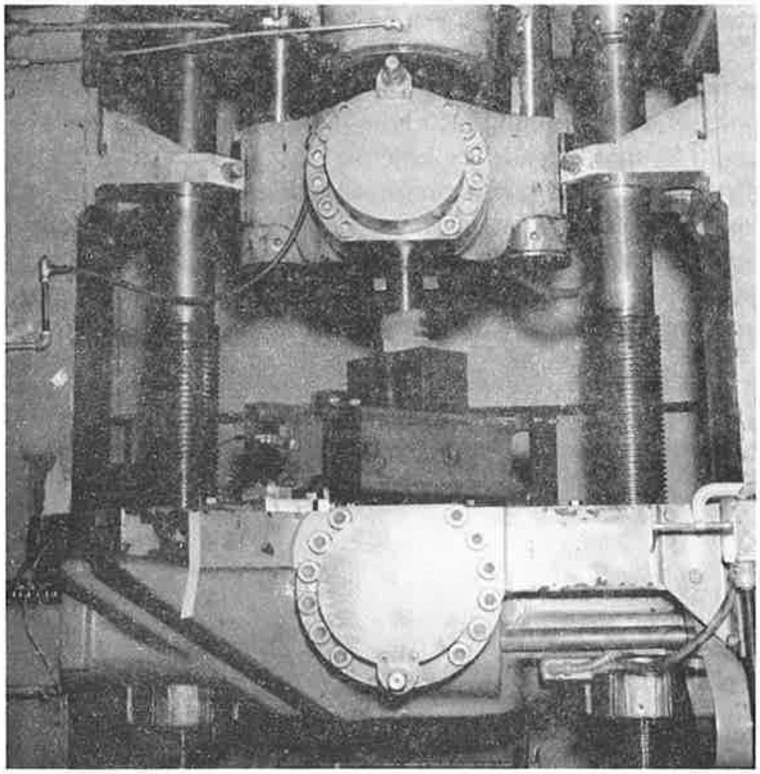

Figure 22.—Rail Fatigue Test Setup

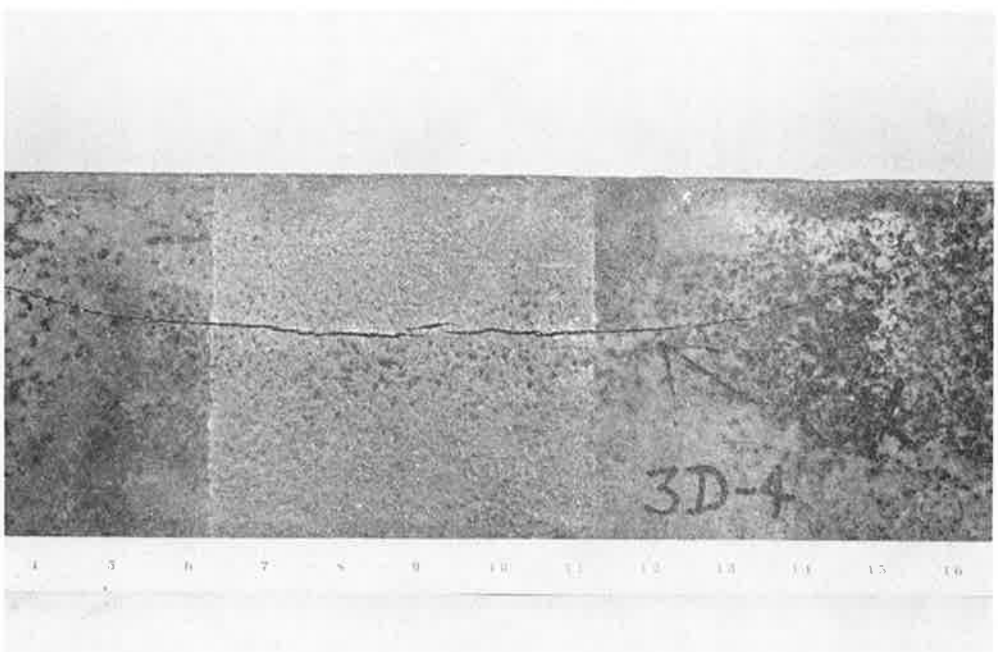

Figure 23.—Base Crack Failure

3.3.3.2 Crack Detection

Each hole on each two-hole specimen was equipped with a crack detector or crack wire circuit (a fine copper wire surrounding each hole, fig. 24) bonded to the web surface. The wire was placed 0.25 inch outside the hole periphery. A crack extending 0.25 inch from the hole broke the crack detection circuit, shutting down the test machine. Thus, all hole failures documented in the test report are nominally 0.25-inch long, unless otherwise noted. The machine used required approximately 600 to 800 cycles to stop after crack circuit interruption. Thus, a rapidly growing crack could grow as much as 0.75 inch before complete machine stoppage. In some cases, total failure of the rail (head-through-base) occurred.

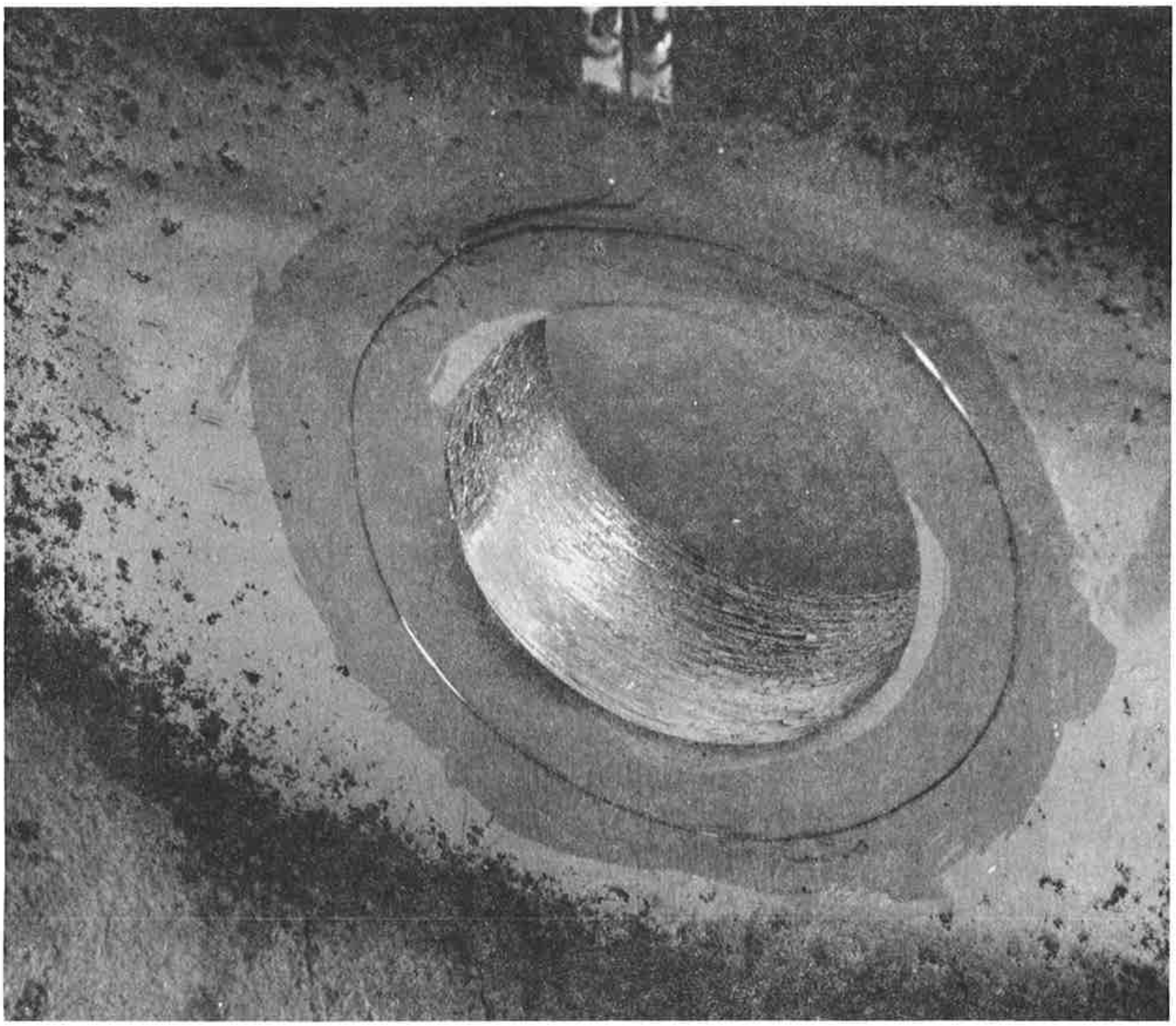

Figure 24.—Crack Wire Circuit

3.3.3.3 Test Procedure

The test procedure followed in conducting the experiment was to develop a stress versus cycles-to-failure curve for the non-cold-expanded and cold-expanded specimens and then select a high and low stress level for testing the remaining specimens of the test matrix.

Tests to determine crack growth rate were conducted on cold-expanded and non-cold expanded specimens. The rail stress analysis and prior test results indicated that hole-crack initiation would occur at an angle of 45° from rail centerline, generally in the direction of the rail head. Consequently, two four-hole specimens (one cold-expanded and one non-cold-expanded) were instrumented with crack-growth-rate detection gages. The gages consisted of a series of parallel wires brought to a junction, forming a portion of the crack detection circuit. The particular gages used (fig. 25) were composed of 20 wires spaced at 0.08 inch, permitting crack growth to 1.60 inches to be studied. Trace readout devices permitted fatigue-machine cycles to be recorded as each wire was failed by the propagating crack.

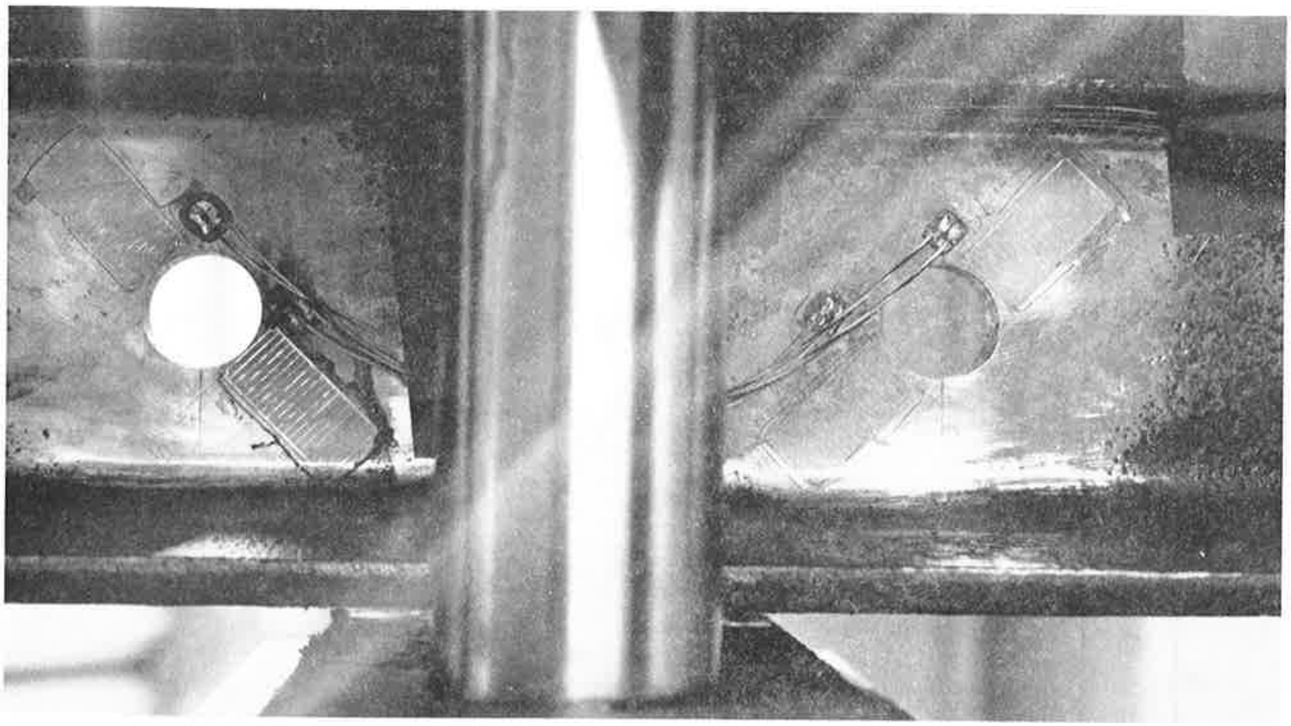

Figure 25.—Crack-Growth-Rate Gages

3.4 TEST RESULTS AND OBSERVATIONS

3.4.1 STRESS VERSUS CYCLES TEST

Two-hole specimens fabricated from rail No. 3 (table 1) were tested to develop a stress-versus-cycles curve for selection of the high and low stress levels to be used for the matrix tests (sec. 3.2.1 and table 6).

As shown in figure 26, no hole-initiating failures could be obtained in cold-expansion specimens at less than a 170-kip load level. Even at this load, 6 x 10^6 cycles were required to produce failure. Consequently, a 170-kip load level was selected for the remaining Task III (sec. 3.0) tests. Also, due to schedule limitations, and anticipating some failures in the 1 x 10^6-cycle region, it was not possible to cycle all cold-expanded specimens to failure. As a result, the tests were limited to the 1- to 2-million-cycle region. The information from unfailed specimens was not lost in that it was used in the statistical analysis of test results.

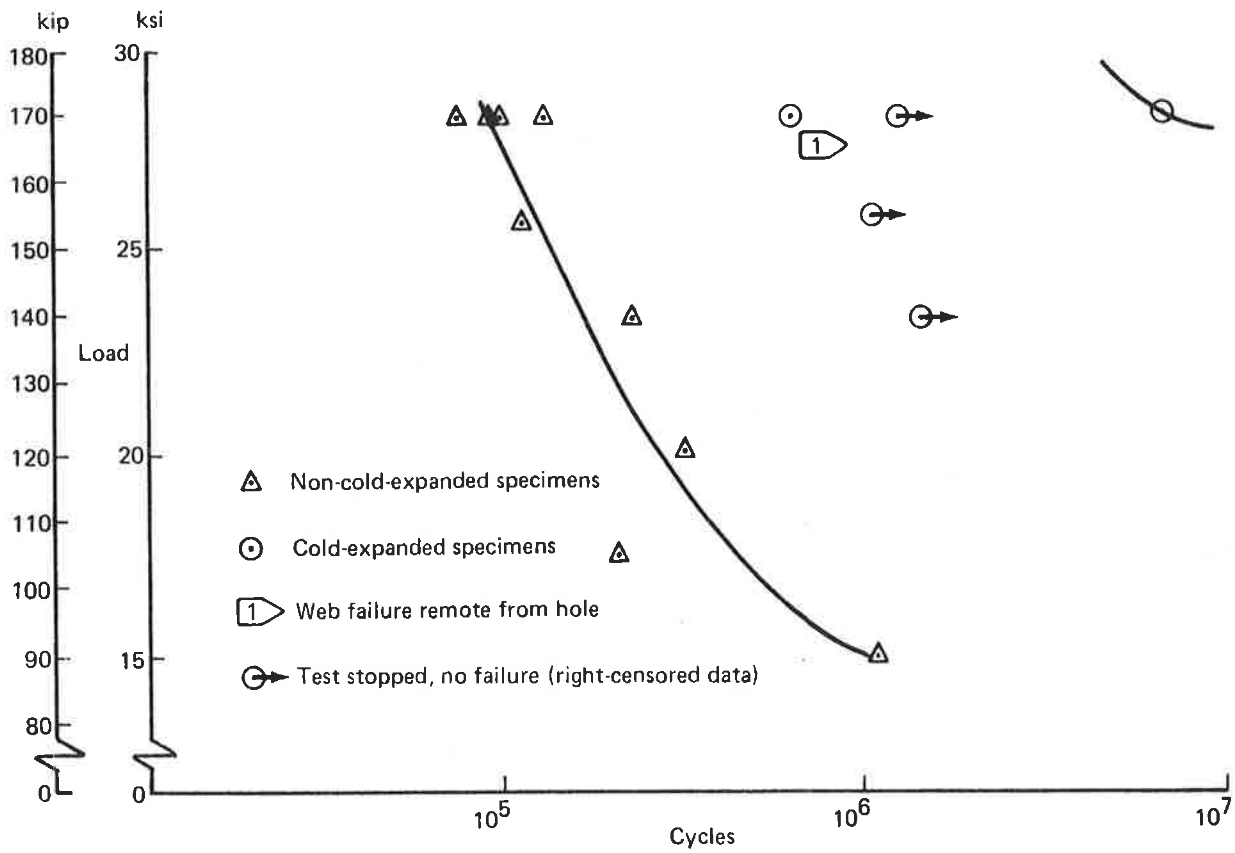

Figure 26.—Rail Specimen S-N Curve

3.4.2 NONFRETTED TESTS

The results of the nonfretted tests (shown in appendix C and fig. 27) indicate that the improvement in fatigue performance resulting from sleeve cold expansion is considerably greater than originally anticipated. The life improvement appears to be one or more orders of magnitude at high stress or load levels, and is anticipated to be considerably more at the lower stress levels encountered in service. In terms of endurance limit, the cold-expansion process produces nearly 100 percent improvement.

The 170-kip load used during this accelerated testing is many times the wheel loading encountered in service; however, the test did demonstrate correlation to rail-failure history. All non-cold-expanded specimens failed at the bolt hole (fig. 28), a frequent failure point for in-service rail. All cold-expanded specimens exceeded 1×10^6 cycles or failed at a point remote from the bolt hole. This suggests that cold expansion of rail bolt holes would reduce the failure rate to the level of those failures not associated with the bolt hole.

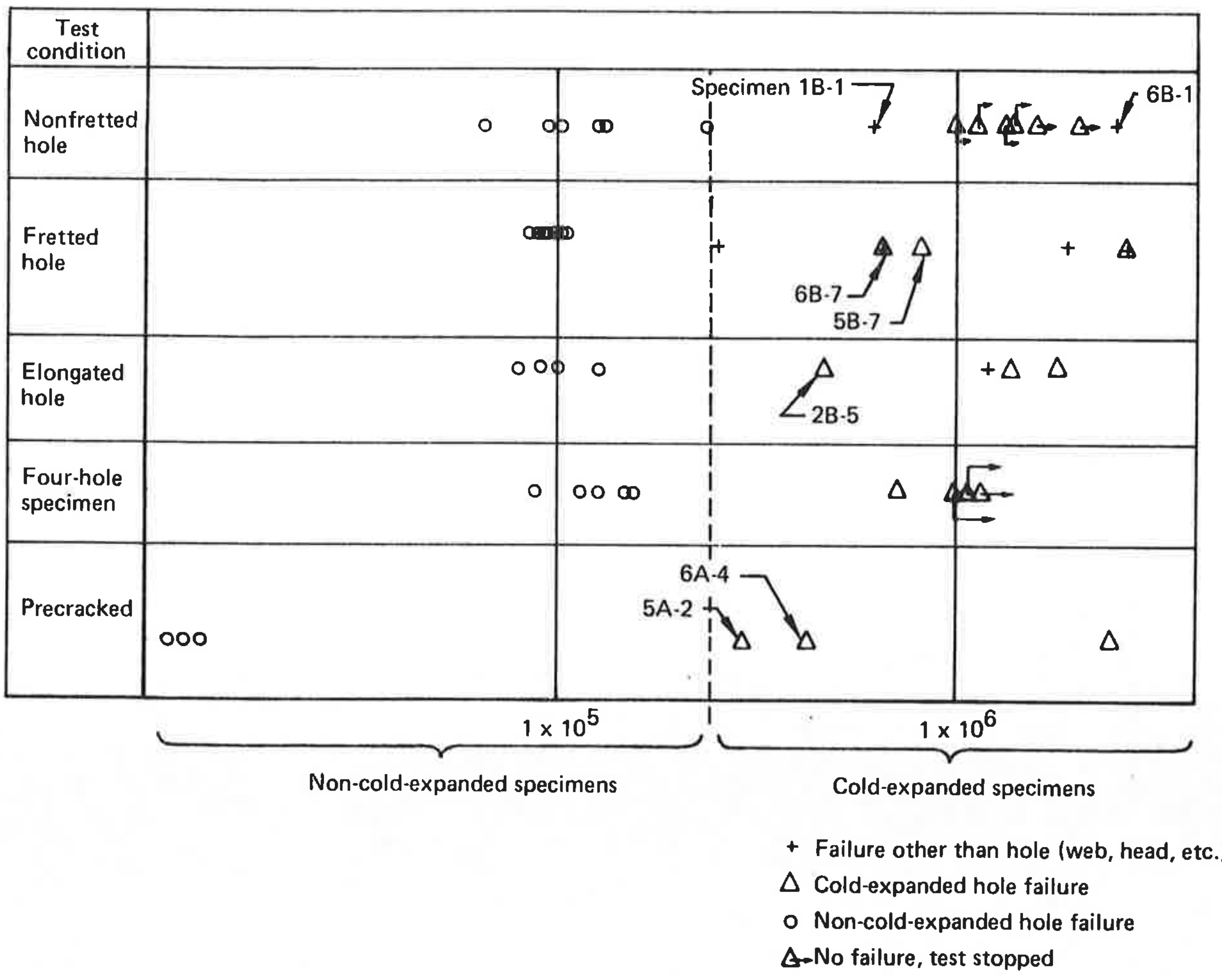

Figure 27.—Test Conditions/Cycles to Failure

Data in appendix C show that cold-expanded specimen 1B-1 (fig. 27) displayed web failure at 643,820 cycles, the first cold-expanded-specimen failure to occur under 1,000,000 cycles other than the base failures. Accordingly, the specimen was cut open for evaluation of the failure face. The crack was arrayed at an angle of 40^{o} from horizontal rail centerline, extending from the web neutral axis upwards toward the rail head. Crack initiation occurred at the web surface near the point of minimum web thickness and progressed in both directions, toward the head and toward the hole (fig. 29). The crack progression toward the hole intersected the crack detection circuit, stopping the test. The crack initiation occurred just outside the area of maximum anticipated hole cold-expansion effect, as estimated by rust removal during the cold-expansion process. No obvious metallurgical defects were noted.

A second specimen, 6B-1 (fig. 27), which was allowed to exceed 1,000,000 cycles, failed at 2,338,530 cycles with failure initiation occurring in the rail head (fig. 30). The remaining six cold-expanded specimens of the nonfretted tests had not failed when tests were terminated at 1- to 2-million cycles.

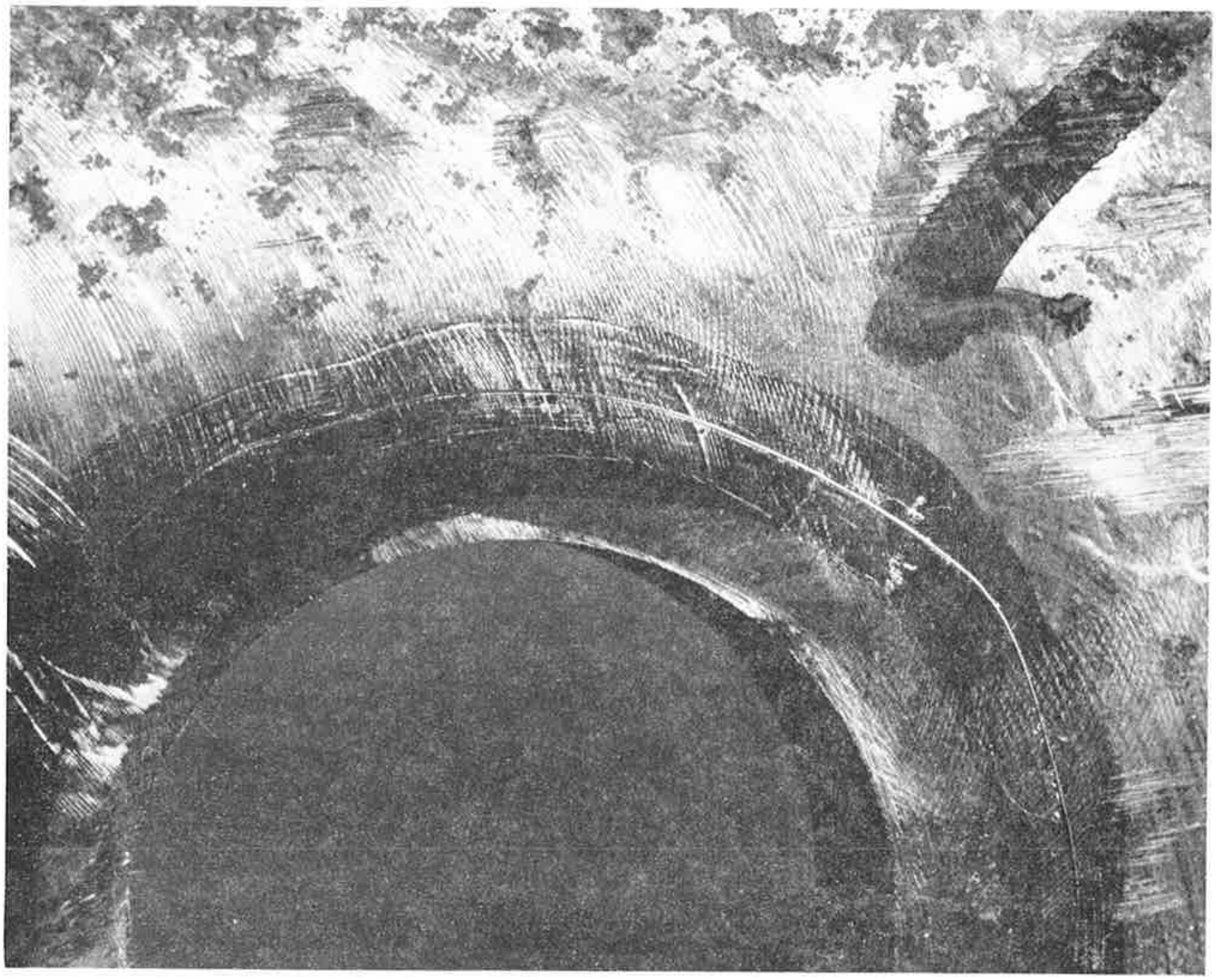

Figure 28.—Bolt-Hole Failure

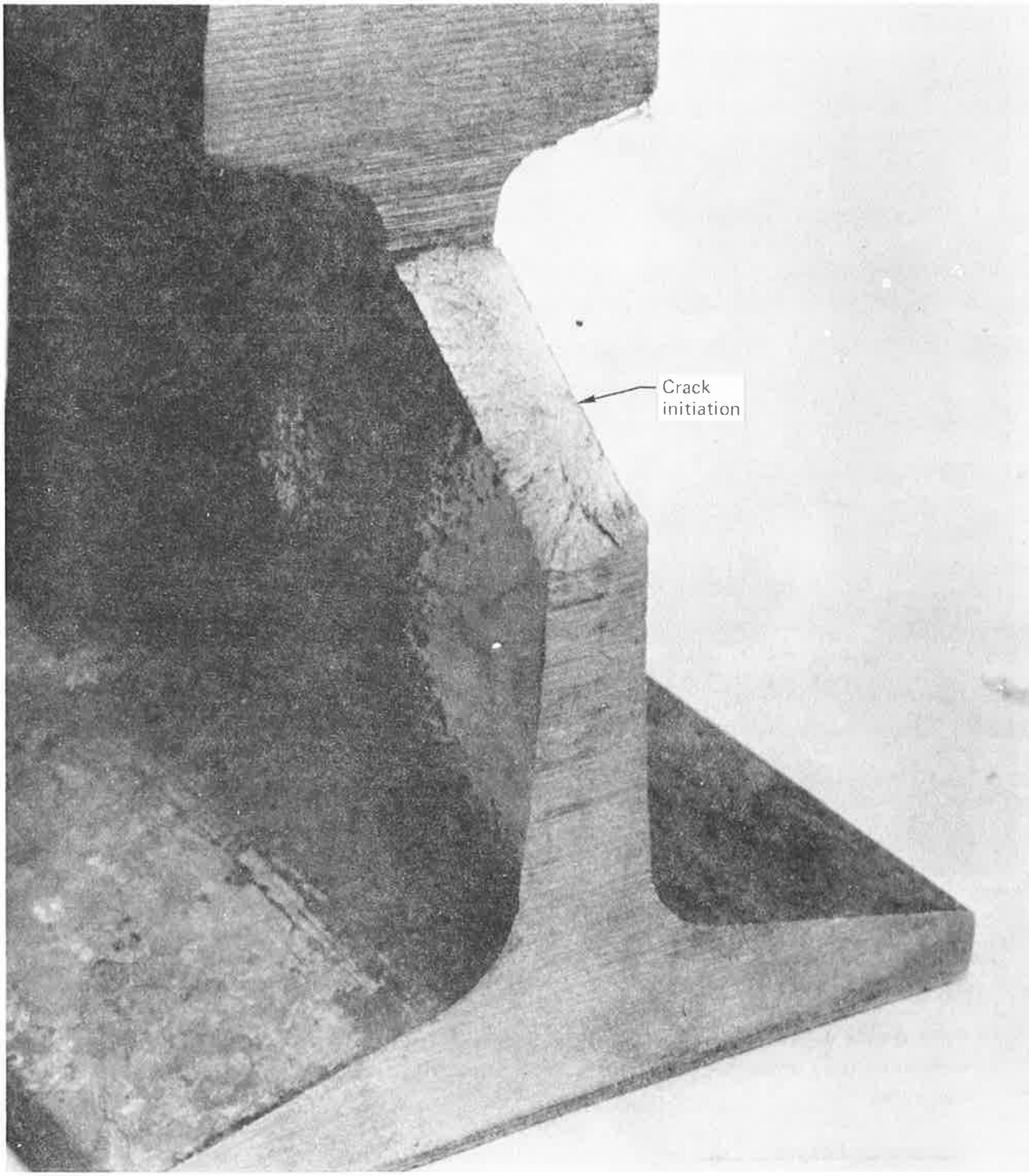

Figure 29.—Web Failure

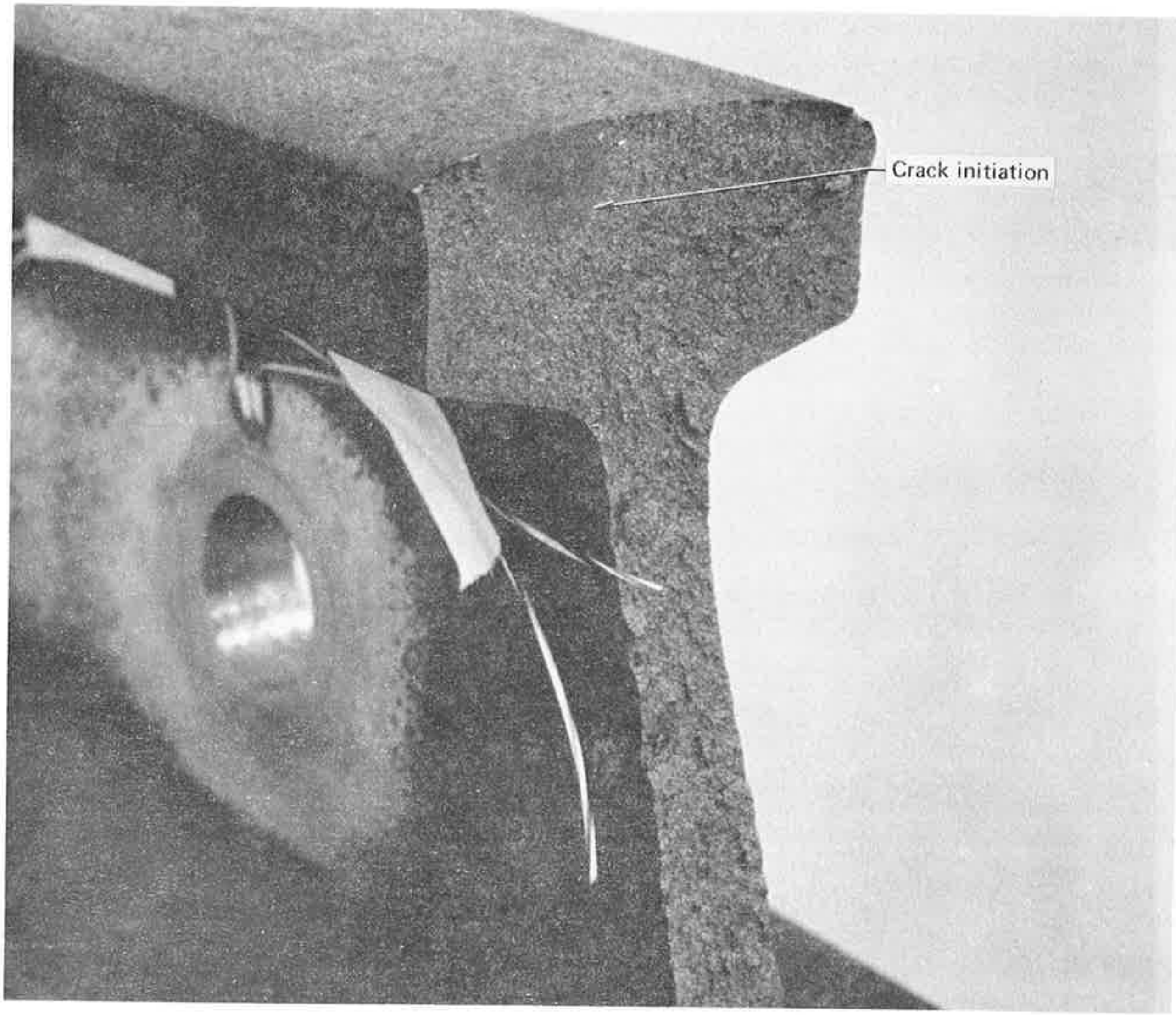

Figure 30.—Head Failure

3.4.3 FRETTED TESTS

Fretted tests were conducted as described in section 3.3.3.1. The turnbuckle strain gages were monitored throughout the fatigue tests. Very little deviation from the 8-kip load was noted.

The non-cold-expanded specimens consistently failed at the hole, with little variation from 100,000 cycles. The cold-expanded specimens were equally divided between web and hole failures. The impact of fretting is demonstrated by specimens 5B-7 and 6B-7 (fig. 27), as these were the first cold-expanded specimens to fail at the bolt hole at less than 2×10^6 cycles. Figure 31 illustrates the web failure mode encountered with fretted cold-expanded specimens. Figure 32 shows a typical fretted specimen hole failure (0.25-inch-long crack).

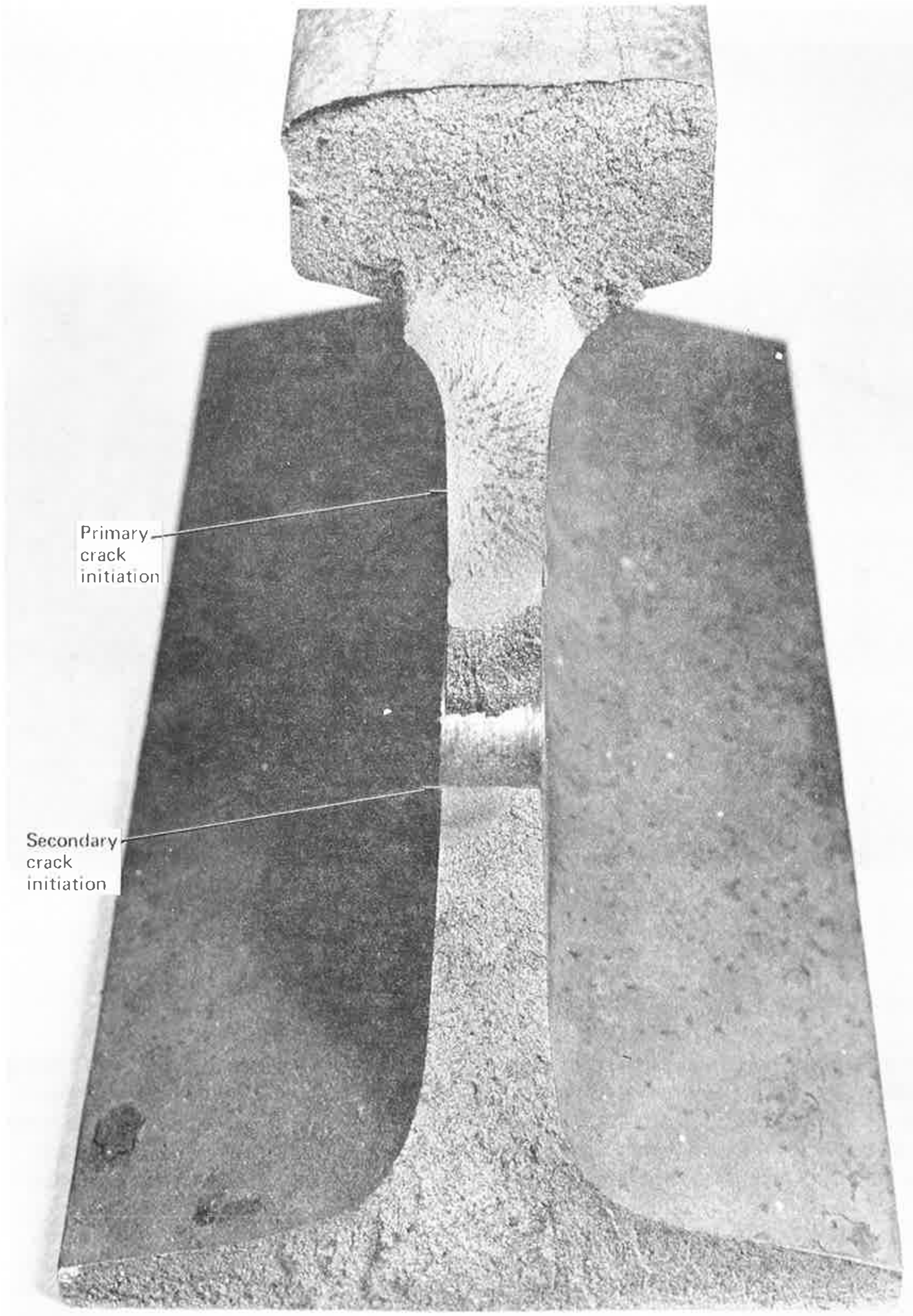

Figure 31.—Fretting Specimen Web Failure

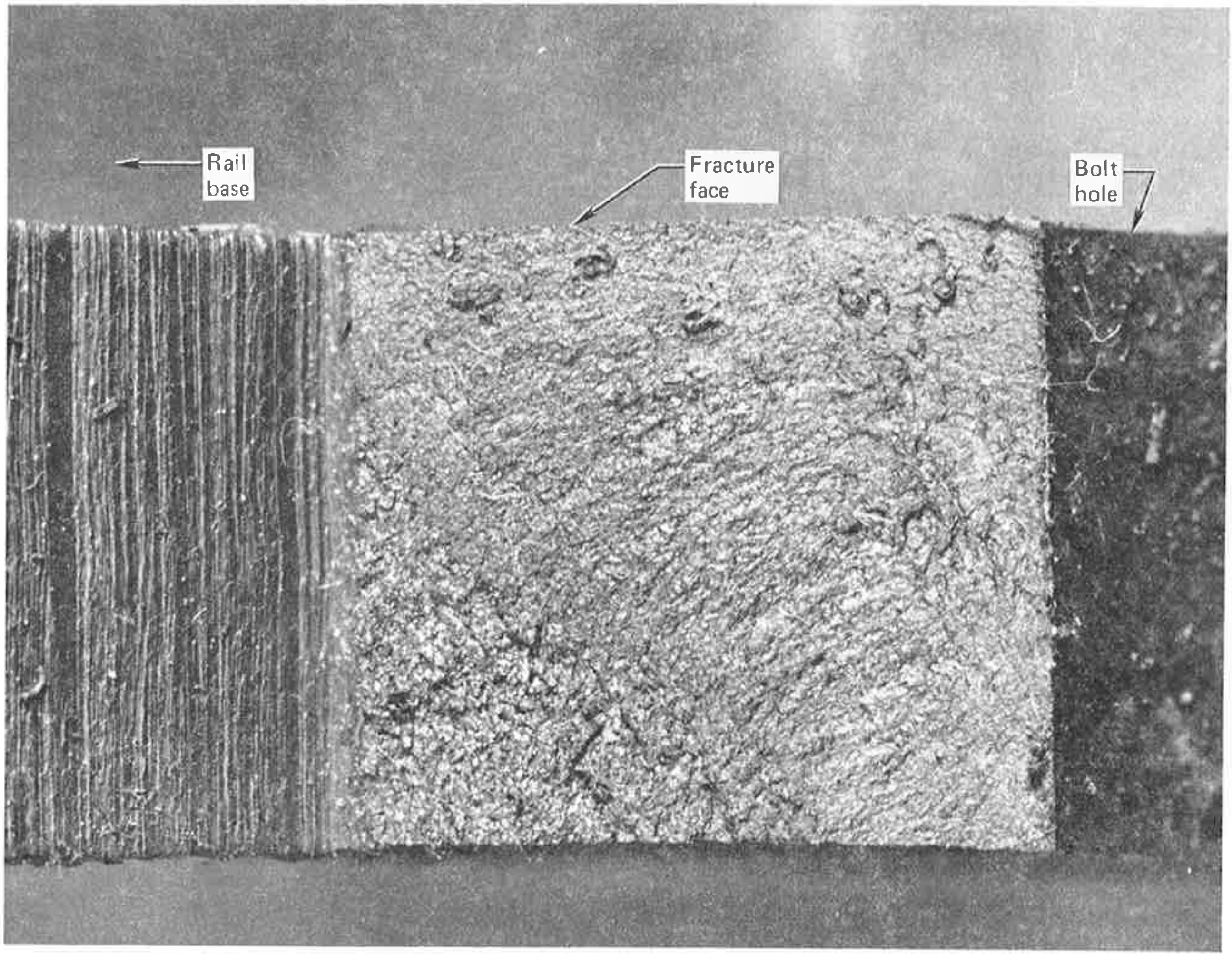

Figure 32.—Hole-Initiated Failure in Cold-Expanded, Fretted Specimen

3.4.4 PRECRACKED TESTS

The precracked specimens, described in section 3.3.3.3, were tested at the normal (170-kip) loading. No fretting device was used. The results, appendix C, indicate a near 10-time reduction in crack-growth rate for the cold-expanded specimens. The crack detection system on specimen 6A-4 (fig. 27) was interrupted by a head-to-radius crack when the precrack was only 0.53-inch long. Specimen 5A-2 also failed at a relatively low number of cycles.

3.4.5 ELONGATED-HOLE TESTS

Four cold-expanded and four non-cold-expanded specimens were loaded with a tensile fixture, using 1-inch-diameter high-strength bars located through the bolt holes, as described in section 3.3.3.2. Tensile loads (table 7) sufficient to cause yielding of the hole then were applied, followed by fatigue testing in the normal fashion without fretting devices. Results are shown in figure 27. Tabulated data are shown in appendix C and the degree of bolt-hole elongation in table 8, section 3.3.3.2. Cold-expanded specimens exceeded 10^6 cycles with the exception of specimen 2B-5. No specific reason for the relatively low number of cycles of this specimen was discovered.

3.4.6 FOUR-HOLE SPECIMENS

Four cold-expanded and four non-cold-expanded specimens drilled and worked to the same procedures used on the two-hole specimens, were fatigue tested to ensure that a different rail hole pattern would not alter the effect of hole cold expansion. As indicated by the data shown in figure 27 and appendix C, the life improvement of the cold-expanded four-hole specimens, as compared to four-hole non-cold-expanded specimens, was similar to the comparative improvement of the two types of two-hole specimens. These tests substantiated the state of stress data (sec. 3.3.1), in that all failures occurred in one or the other of the two center holes.

3.4.7 CRACK-GROWTH-RATE DETERMINATION

Test results of the non-cold-expanded specimen 5A-5 are shown in figure 33.

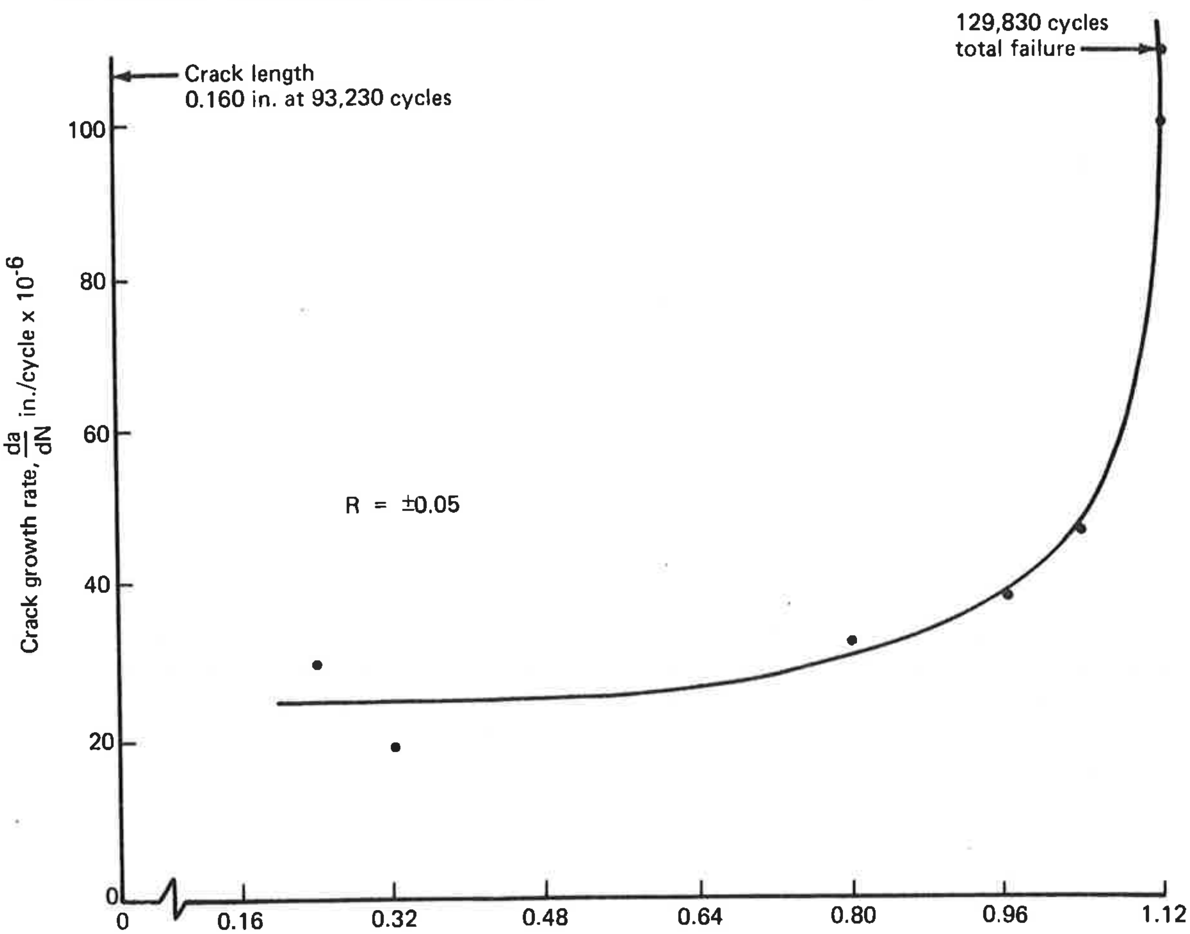

Figure 33.—Crack Growth Rate

The cold-expanded specimen (5B-5) achieved 1,277,000 cycles before failure of the first gage wire (crack length = 0.080 inch). However, a 4-inch-long crack had developed in the rail web as indicated in figure 25, preventing further testing of this specimen. A second cold-expanded specimen tested disintegrated at the end hole at 600,000 cycles, prior to any indication of failure of the two center, gaged holes.

3.5 STATISTICAL ANALYSIS AND CONCLUSIONS

The data generated by the laboratory tests on 112-lb rail (described in sec. 3-1 through 3-4) were statistically analyzed to evaluate the effectiveness of cold-expanding bolt holes. The rail life was assumed to be governed by a two-parameter Weibull distribution (ref 6). If the life of a rail in cycles is Y, then the probability (p) that the life is greater than y (the reliability function at y) is given by

$$p(Y > y) = \exp - (y/A)^B$$

where A is the scale parameter and B is the shape parameter. Examination of the data through reliability plots supported this assumption (e.g., fig. 34).

The data were analyzed by taking the natural log of the cycle data:

$$X = \text{Ln } Y = \text{log life time}$$

This yields the double exponential reliability function governing log life:

$$p(X > x) = \exp[-\exp((X-L)/D)]$$

where L is the location parameter and D is the scale parameter. The relationship between the parameters of these reliability functions is:

$$D = 1/B$$

$$L = \text{Ln } A$$

Transformation to log cycles permitted use of efficient estimation techniques to evaluate the data. Maximum-likelihood estimates of the parameters were obtained through an interactive Newton-Raphson procedure (ref 7).

It was planned that at least some of the test rails would be right censored. That is, they would be allowed to run either until they failed, or until a fixed number of cycles, (e.g., 10^6) had been obtained and the rail did not fail and was thus censored. Although accelerated life testing was being used (higher loading than normally seen in the field), some specimens might run for a long time before failing, increasing flowtime of the experiment. The statistical procedures permitted full use of information from right-censored data to estimate the reliability-function parameters.

---

[6] Mann, N. R., et al., *Methods for Statistical Analysis for Reliability and Life Data,* Wiley and Sons, 1974.

[7] Wagner, H., *Principles of Operational Research,* Prentice-Hall, 1969.

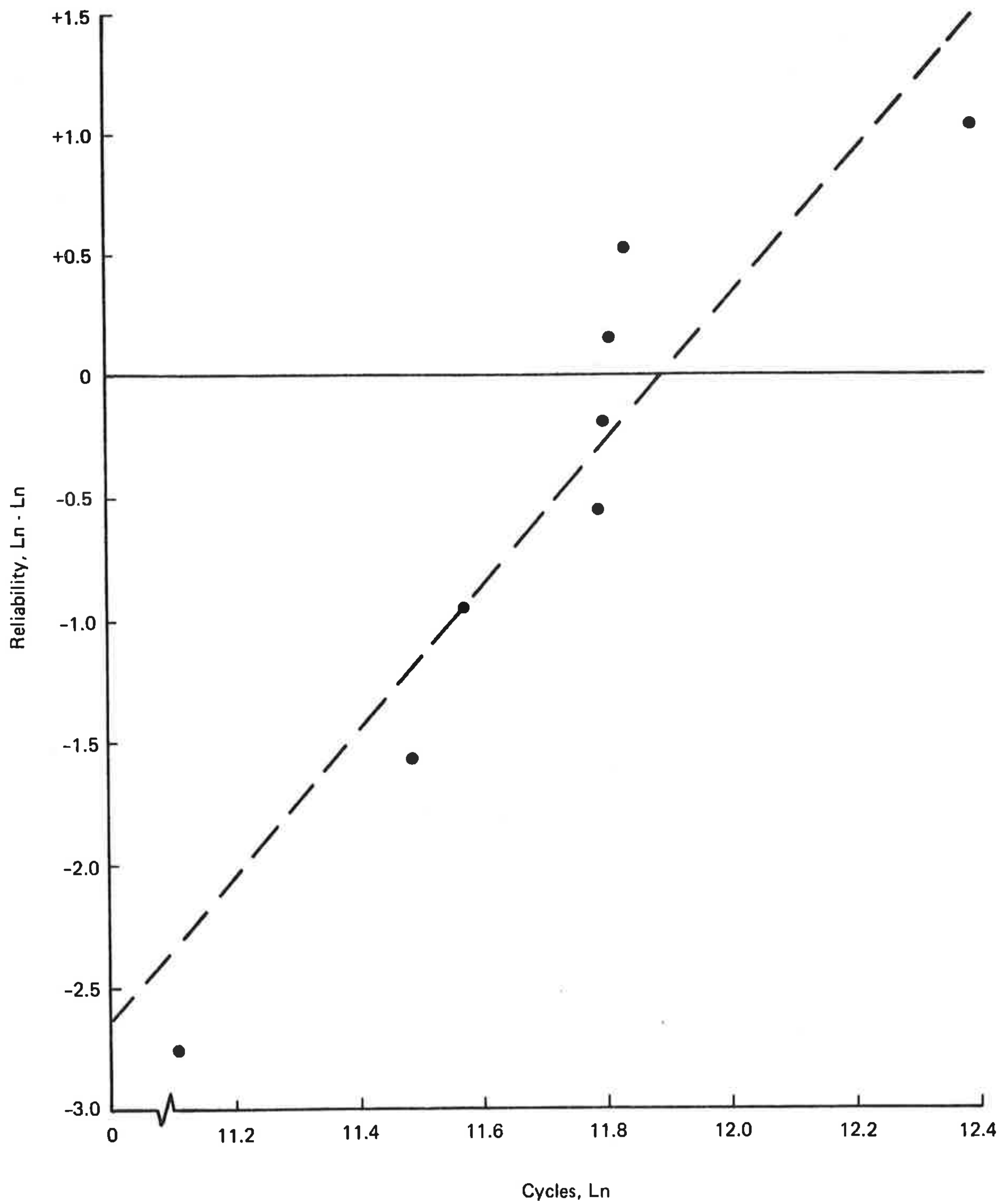

Figure 34.—Reliability Plot

In life testing, it is common to assume that shape parameter D (the inverse of the slope in the reliability plot) is the same for the two populations. This permits comparison of two populations by comparing the location parameters L. The expression exp $(L_A - L_B)$ estimates the ratio of expected lifetime A to expected lifetime B for A and B to achieve the same reliability R and is independent of R.

The Ds were tested for equality using a likelihood-ratio test. Only for the fretted test was the assumption of D equality between cold-expanded and non-cold-expanded rails rejected. When the Ds are the same for cold-expanded (CE) and non-cold-expanded (NCE) specimens, the quantity exp $(L_{CE} - L_{NCE})$ estimates the "improvement in life" for all reliability values. This is the factor increase in expected life for cold-expanded over non-cold-expanded to achieve the same reliability. The Ls are the maximum likelihood estimates for cold-expanded and non-cold-expanded specimens. "Improvement in life" has been tabulated for each of the treatments (table 9). For example, in the first row of the test matrix (table 6, sec. 3.2.1), the Ds were found to be not significantly different and $L_{CE} = 15.19$, $L_{NCE} = 11.84$, yielding the improvement of life when cold-expanded as exp $(15.19 - 11.84) = 28.5$. If the non-cold-expanded specimens have a 90% reliability after 53,000 cycles, the cold-expanded specimens have a 90% reliability after 28.5 x 53,000 cycles, or 1,500,000 cycles.

For fretted specimens, the Ds were found to be significantly different. Comparing the two populations at the 90%-reliability points showed that cold-expanded specimens lasted 3.5 times as long as non-cold-expanded specimens. Comparing them at their 50%-reliability points showed this ratio as 6.6. Also, note that when the untreated specimen has degraded to 50% reliability, the cold-expanded specimen is at 98% reliability.

Table 9.—Test Results Reliability Summary

Treatment	Rail type	Parameters L	Parameters D	Expected life	90% reliability	Improvement in life
Nonfretted	CE NCE	15.19 11.84	0.43 0.43	3,502,000 123,000	1,500,000 123,000	28.5
Fretted	CE NCE	14.22 11.56	0.67 0.05	1,353,000 102,000	335,000 93,000	Not applicable 1
Precracked	CE NCE	14.02 8.41	0.72 0.72	1,120,000 4,100	243,000 900	271.0
Elongated	CE NCE	14.26 11.59	0.25 0.25	1,413,000 98,000	884,000 61,000	14.5
Four hole	CE NCE	14.13 11.87	0.21 0.21	1,255,000 131,000	847,000 88,000	9.6

CE—cold expanded

NCE—noncold expanded

1 Ds were significantly different between CE and NCE.

Although it would be desirable to make quantitative projections from the laboratory tests to the expected results in the field, such a projection would be highly questionable. The mechanism by which rail is loaded in the laboratory is not the same as that in the field, and the load used is many times greater than that usually observed in the field.

The purpose of accelerated life tests is to achieve meaningful comparisons within a short period of time. Although the "improvement in life" may not be what is observed in the field, the effects of the various treatments should stay roughly in the same relation.

4. TASK IV—FIELD EXPERIMENT

4.1 PLANNING THE FIELD EXPERIMENT

To effectively plan the field demonstration of cold-expanded rail bolt holes, it was essential to gain a better understanding of the operating system of a U.S. railroad. Boeing obtained a working arrangement with a major railroad that made it possible to study parts of their rail system. A proprietary data base detailing a 3-year record of all rail failures was obtained, as was a full description of the existing track. Time was spent with some of the key railroad personnel to learn how changes in track maintenance and relaying decisions are made. Through this interaction with the railroad, an appreciation was developed for their concerns about current track conditions and operation problems expected in the near future. It was found that they also were faced with major data problems, in that more data was being accumulated than they were using, yet less than necessary for investigating and predicting future effects under various scenarios.

Their data base suggested that most of the rail-bolt-hole failures in the last year were in 112-lb or lighter rail. However, this weight rail is used for a large percent of their (and U.S.) existing track. Money and time were not available to replace this track with heavier weight rail over system areas with dynamically increasing load, making failures inevitable.

A section of straight track with an appreciable and increasing bolt-hole-failure rate was sought for a field demonstration of cold-expansion. However, those found by Boeing were not of prime interest to the railroad. They knew of another area with a lower failure rate that would experience a dynamic increase in annual gross tonnage, greatly increasing the failure rate.

4.2 PLANNING THE UNION PACIFIC FIELD DEMONSTRATION

The Union Pacific Railroad was contacted and they expressed a strong interest in participation in a demonstration of the feasibility and utility of cold expanding existing rails in service. They felt that this process would be of help to them in the manufacture of switches and frogs because these items would continue to be bolted in the future. Union Pacific located an area with a history of bolt-hole failures that was not scheduled for major servicing or to be relaid in the near future. The selected site at Silver Creek, Nebraska, has straight parallel east- and west-bound tracks, thus, treating the rail could be accomplished without interrupting service.

Examination of rail-failure data from this area (table 10) showed an appreciable bolt-hole-failure rate, which Union Pacific felt was increasing. Table 10 identifies the pretest incidence of bolt-hole-failure rate as referenced to the treatment implemented in the experiment.

Table 10.—Pretest Incidence Rates for Test-Area Track (January 1972—December 1975)

Planned treatment	Milepost	Bolt-hole failures	Distance (miles)	Failure rate/ mile year
None	101.00–103.00 112.25–115.00	33	3.95	2.09
Joints cleaned	100.00–101.80 111.00–112.25	14	3.05	0.92
Broached	103.00–104.00 105.00–106.00 106.11–107.00 109.00–110.00	27	3.89	1.39
Cold expanded	104.00–105.00 106.00–106.11 107.00–109.00 110.00–111.00	29	4.11	1.41

A statistically designed experiment was planned for the Silver Creek site. The selected experimental design for this site had to meet the following requirements:

- A data base that could be objectively evaluated, yielding unbiased results
- Easy implementation
- Flexibility to overcome complications in field work.

An idealized design would be to use each rail as its own control. One end would be cold expanded and the other end untreated; treated ends would be balanced, half on one end, half on the other end. This design suffers several practical drawbacks: it is extremely difficult to implement; field crews would require very close supervision; and recording of treated ends, and subsequent failure data, would be prone to error.

The following paragraphs describe the basis for establishing the experimental statistical design. Mileposts, the railroad's method of delineating sections of track, were used to define the experimental plots.

Occurrence of hole elongation in some used rails required that holes be rounded through broaching prior to cold-expanding. Thus, to permit full evaluation of the results, the experimental design had to allow for three treatments; untreated, broached only, and broached plus cold expanded. Then, if the cold-expanded rails showed a significantly lower failure rate, the effect of broaching could be removed.

One mile was established as the smallest unit for each treatment. (There was one deviation from this unit in actual tests.) Alternating miles between treatments permitted balancing of environmental biases. Ideally, all three treatments should be alternated in a balanced array. However, since the control rails were untreated, leaving half of them at each end of the test plot minimized the distance, and hence time, required to move the equipment and complete the field testing.

The relationship between size of the treatment areas and length of study required to obtain significant data was arrived at by the following rationale. The test area was divided into three groups:

1. N_{CE}—miles of railroad to be cold-expanded (CE)

2. N_B—miles to be broached (B)

3. N_U—miles of control or untreated (U) rail.

These three treatments could then be pairwise contrasted. For the CE/U comparison after a period of time (T years), X (number of cold-expanded failures) CE rails and Y (number of non-cold-expanded failures) U rails have failed. The distribution of failures for each test section is approximately Poisson with parameters $T\ N_{CE}\ M_{CE}$ and $T\ N_U\ M_U$ where M_{CE} and M_U and the respective failure rates per mile per year.

If the two parameters are the same, then there is no CE effect. If, however, the CE failure rate is significantly lower than the U failure rate, then M_{CE} would be significantly less than M_U. This reduces to the classical one-sided hypothesis test:

$$H_0 \text{ (null hypothesis)} \quad : \quad M_{CE} = M_U$$

$$H_1 \text{ (alternate hypothesis)} \quad : \quad M_{CE} < M_U.$$

The uniformly most powerful test of this hypothesis is based on the conditional distribution of X, given X + Y, which is a binomial test where P = probability that a failure is cold expanded:

$$H_0 : \text{ X is binomial } (p = 1/2, X + Y)$$

$$H_1 : \text{ X is binomial } (p < 1/2, X + Y),$$

The specification of sample size is based on picking values A and B such that:

1. If H_0 is true, cold expanding has no effect, then A is the probability of falsely asserting that CE is better.

2. If H_1 is true, and $M_{CE} = K\ M_U$, then 1 – B is the probability of detecting this difference.

If X + Y = 40, failures are observed and A = 0.05, the H_0 is rejected if X is less than 15. If $M_{CE} = 1/3\ M_U$, then there is a 5% chance of not detecting the improvement due to CE. If M_{CE} is $1/4\ M_U$, then there is less than a 1% chance of nondetection. This information is related in table 11 to length of study and miles (N) to be treated.

Table 11.—Sample Size Determination

M, failure rate per mile per year \ T, years to observe experiment	1	2	3	4
1.0	50.0	25.0	17.0	12.5
2.5	20.0	10.0	6.7	5.0
5.0	10.0	5.0	3.3	2.5

Note: Miles for each treatment to give 95% assurance of obtaining a sufficient number of failures.

For example, if N = 5 miles is used (5 miles cold expanded, 5 miles control) and the test runs at least 2 years, and if M_{CE} is at least five per mile per year, then the test will give at least 39 failures from the control section alone (with 95% assurance). The section of track identified for test had an annual failure rate approaching five and increasing. Thus, if no failures occur in the CE section, one can assert the improvement due to cold-expanding and attach an appropriate level of significance.

The test results will permit estimation of M_U and M_{CE} and permit putting a lower bound on expected life for CE rails, even if no CE failures are observed. The failure and load data observed as a time series will permit estimation of extreme-value parameters for more precise estimation of future performance, thus not confining to failure rate to be constant. The CE versus B and B versus U comparisons can be similarly performed.

4.3 IMPLEMENTATION OF SILVER CREEK EXPERIMENT

Specifications for the track to be treated at the Silvercreek, Nebraska test site were as follows:

- 15 miles of westbound, 131-pound, six-hole track located between mileposts 100 and 115
- 5 miles of track with joints cleaned and greased
- 5 miles of track with joints cleaned and greased and holes broached
- 5 miles of track with joints cleaned and greased and holes broached and cold expanded.

The experimental design required modification during implementation, necessitated by time, cost (to the railroad), and prototype equipment problems. The cold temperatures encountered during the November test affected the equipment, rails, and joint packing. In addition, a large number of 19-foot rather than the expected 39-foot, lengths were encountered, greatly increasing the number of joints per mile to be treated.

The miles of track receiving treatment are shown in figure 35. Approximately 811 rails were cleaned and greased (3.05 miles); 1071 rails were cleaned, greased, and broached (3.89 miles); and 1129 rails were cleaned, greased, broached, and cold expanded (4.11 miles). Prior to treatment, a detector car covered the area, and all but three detected cracks were removed. Three rails with 1/4-inch-long bolt-hole cracks were cold expanded and left in service. These rails were clearly marked with yellow paint visible outside the joint bars and are to be inspected every 30 days for evidence of crack growth. This inspection will continue for an anticipated 1-year period.

The track sections subjected to different experimental treatments appeared similar with respect to condition of track and environment. Their failure rate per mile per year from January 1972 through November 1976 (when the field test was implemented) were roughly comparable over this time period.

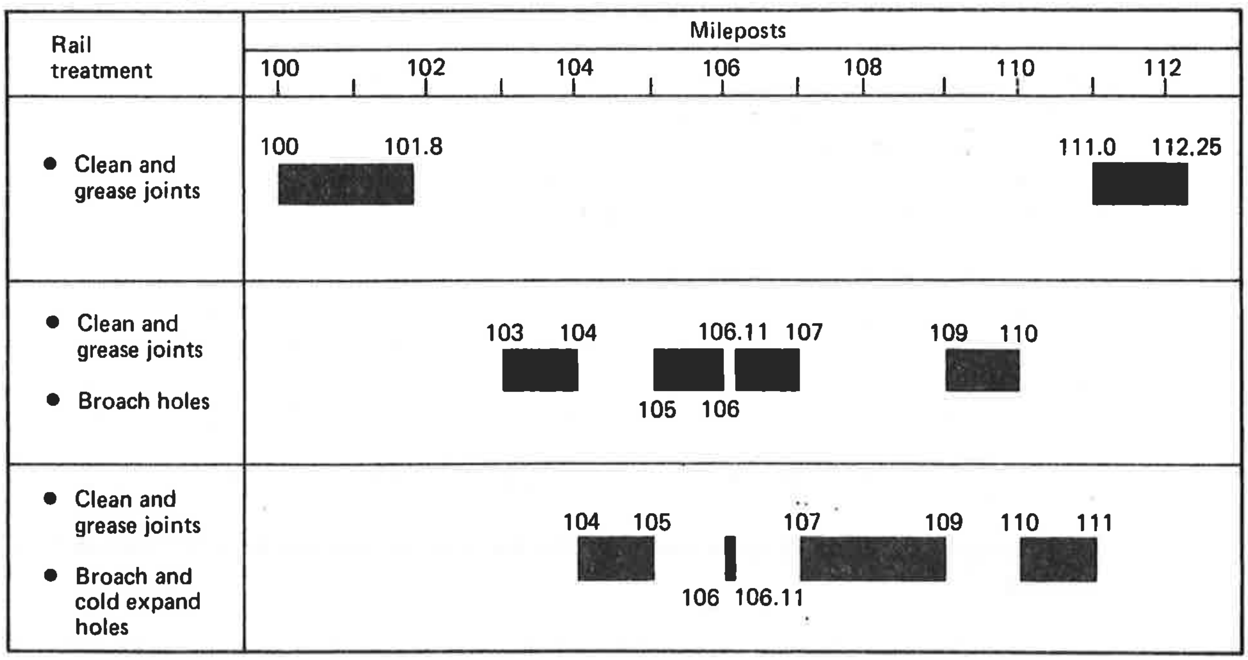

Figure 35.—Updated Test Plan for Silvercreek, Nebraska Site

4.4 DESCRIPTION OF AND OBSERVATIONS ON FIELD COLD EXPANSION

The test, conducted with the direction and support of the Union Pacific Railroad, provided an opportunity to integrate the cold-expansion process as a function of a normal track-joint-maintenance crew.

The crew assigned to this effort consisted of left- and right-hand joint-breakdown crews, left- and right-hand joint-cleanup crews, one joint-lubrication crew, and two joint-replacement crews. The following men were added and followed the second cleanup crew:

1. A reamer (to remove elastomeric packing and grit from rail bolt holes)
2. Broach gun operator, tool handler, and lubricator (fig. 36)
3. Air compressor operator (fig. 37)
4. Cold-expansion gun operator and two assistants, one to load the sleeve and remove the mandrel from the gun, and one to mount the mandrel in the rail bolt hole (fig. 38)

Figure 39 shows the broach pull gun and broach; figure 40, the broach pull gun and power supply; and figure 41, the cold expansion (mandrel) pull gun and power supply. The cold-expansion mandrel and sleeve are shown mounted in a rail cross-section in figure 42.

The basic sequence of operation was as follows. As the wire-brush machine used by the second-in-line cleanup crew was moved forward to clear the joint area, the six holes of the joint (either right or left hand) were reamed with a 1-1/4-inch-diameter reamer, driven by a 75-foot line from the air compressor. The reamed 1-1/4-inch-diameter-hole size, the standard for this track section, was the planned starting-hole size for the broach operation. The reaming operation was intended only to remove grit from the hole, not to size it. The hand-held reamer was far too slow in operation to remove more than 0.001 to 0.002 inch from the bolt-hole bore. Where hole sizes under 1-1/4-inch diameter were encountered, these holes were drilled to 1-1/4-inch diameter using a conventional track drill.

The broach operation employed two broach tools and one broach pull gun; one man inserting one broach in the next bolt-hole bore while the second broach was being pulled through the previous hole, thereby increasing hole diameter to the 1-5/16-inch starting-hole size for cold expansion (table 3, sec. 2.0). The third man brush-applied cutting oil to the broach as it was being pulled through the bore. Time lapse from hole to hole averaged 22.5 seconds, including all delay time other than that required to move the compressor and crew from joint to joint and the delay when the track was cleared for traffic on the eastbound track.

The air compressor (a wheeled, diesel-powered, 600-cfm unit maintaining a constant 115-pound air pressure) was arranged between the broach station and the cold-expansion station, permitting simultaneous operation of both pull guns. The air-operated hydraulic power supplies for the two pull guns were mounted for convenience on the sides of the air compressor.

Figure 36.—Broaching Track Joint Holes in the Field

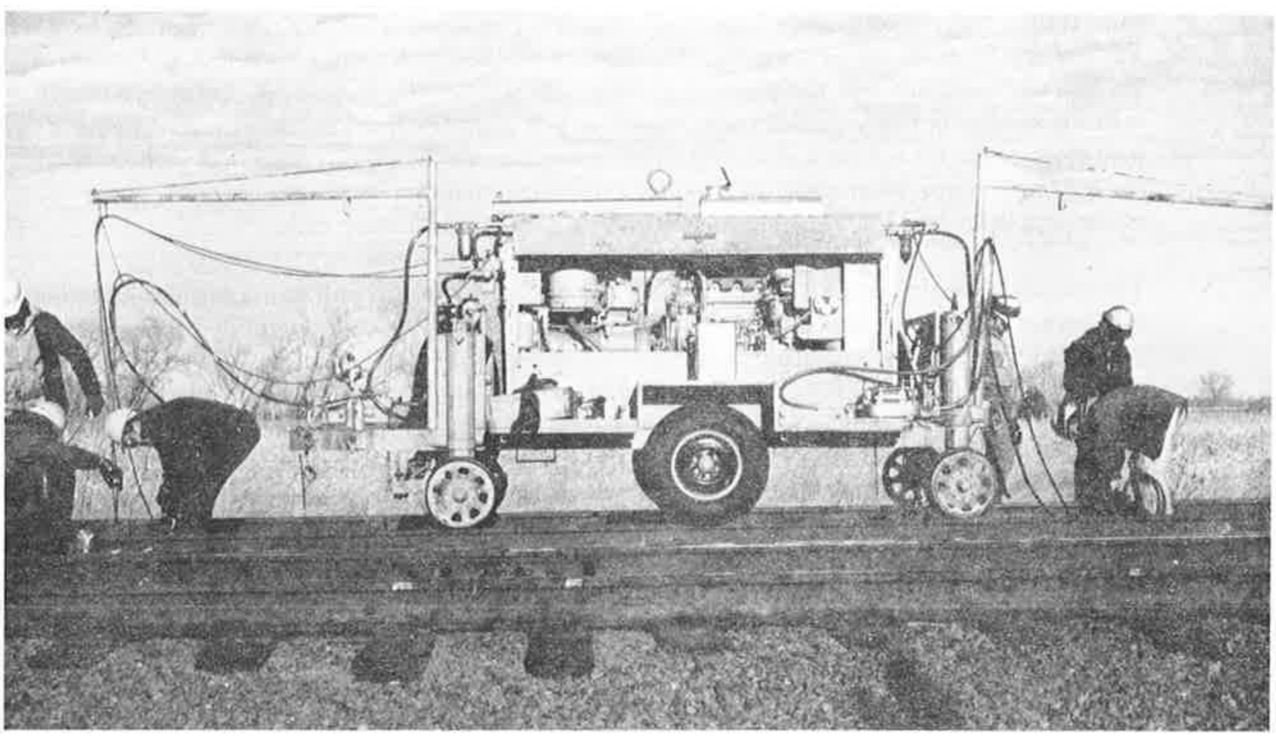

Figure 37.—CP805 Power Supply on Mobile Air Compressor

Figure 38.—Cold Expanding Joint Holes in the Field

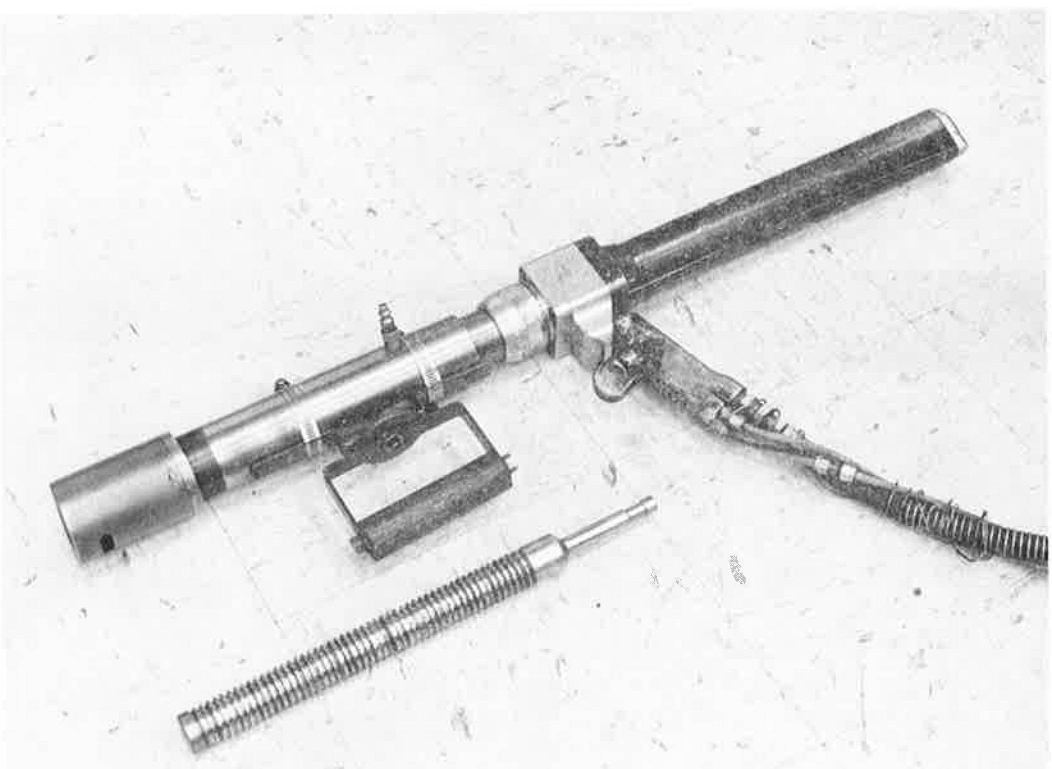

Figure 39.--Broach Pull Gun and Broach

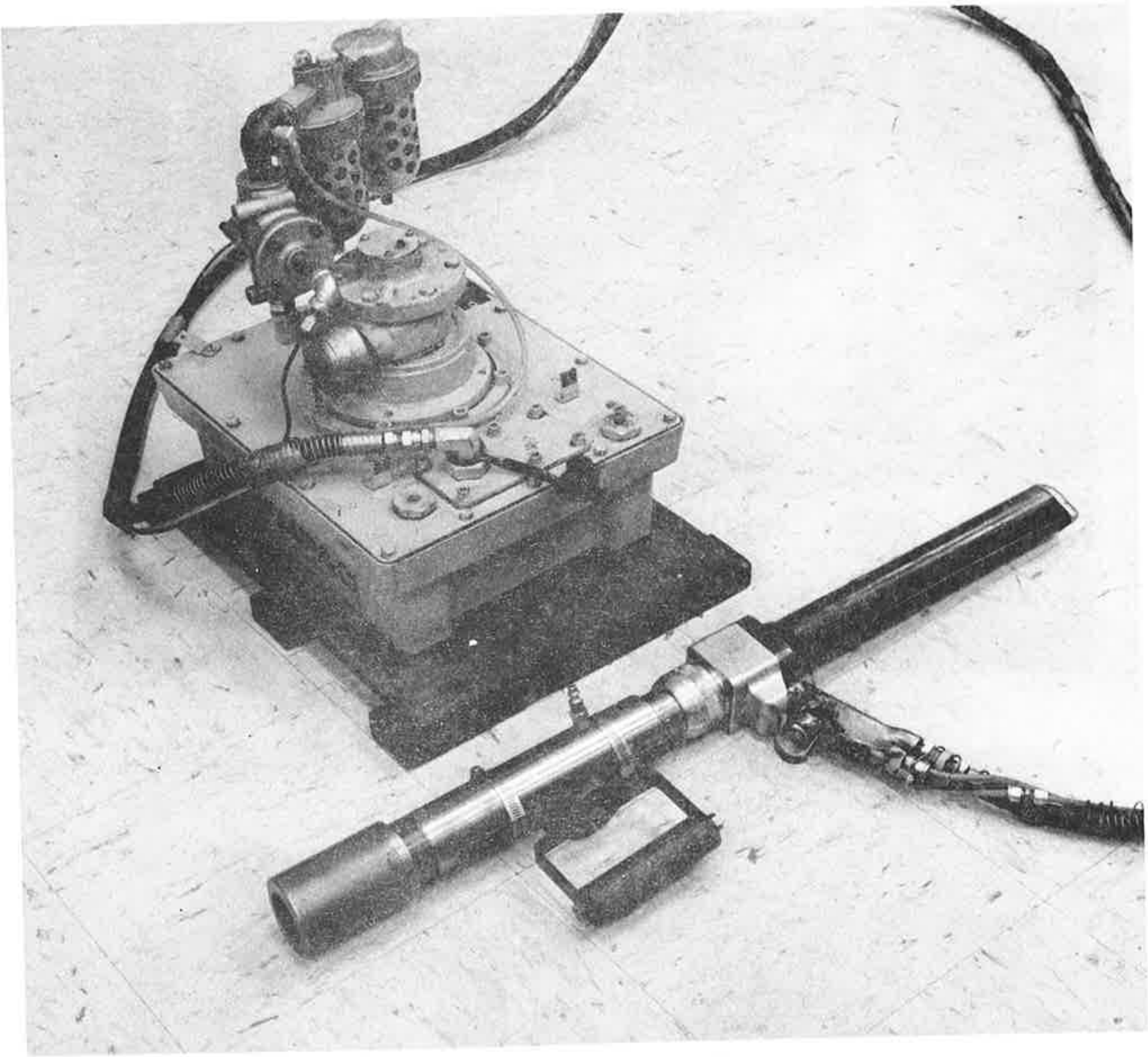

Figure 40.—Broach Pull Gun and Power Supply

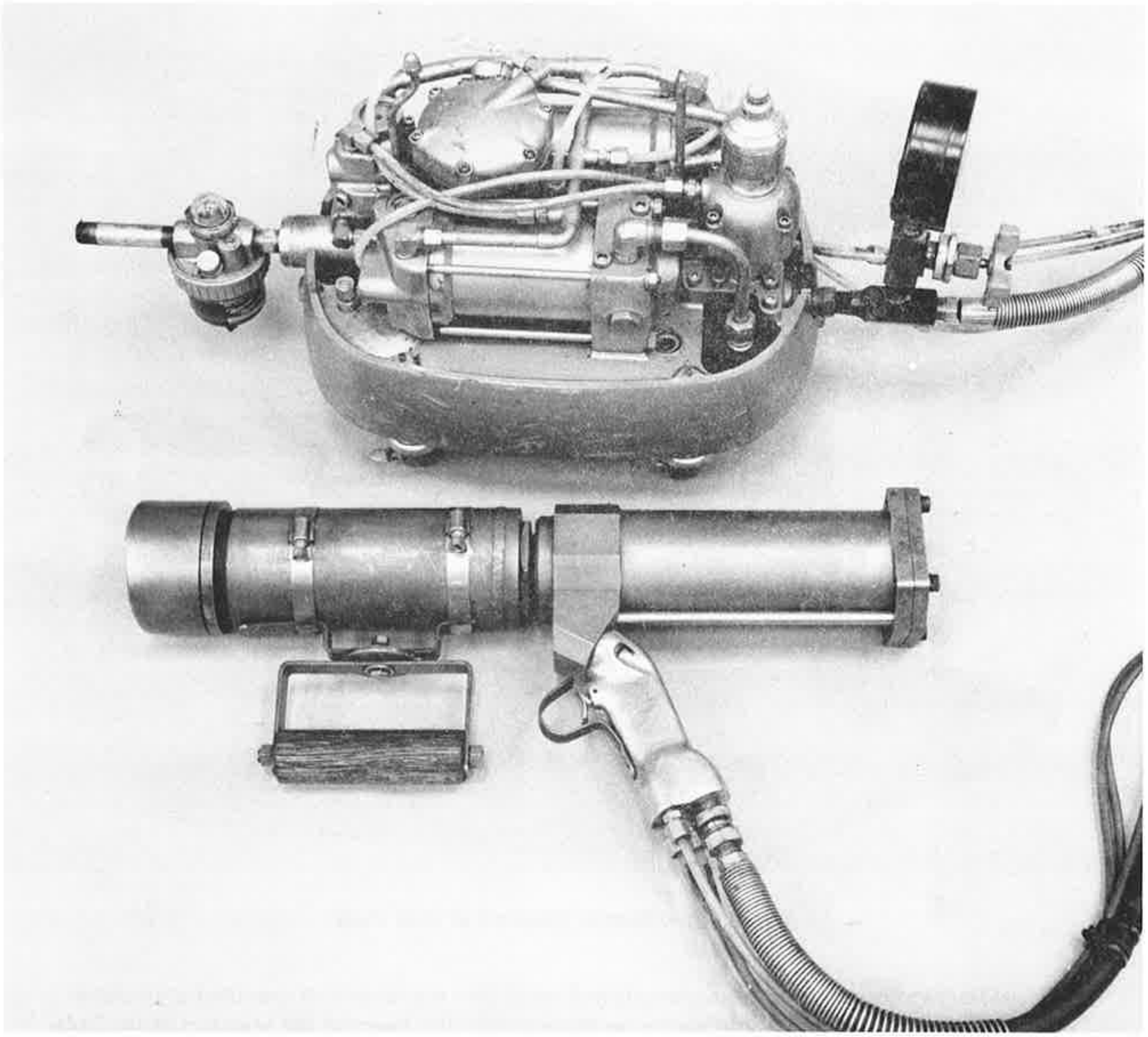

Figure 41.—Cold-Expansion (Mandrel) Pull Gun and Power Supply

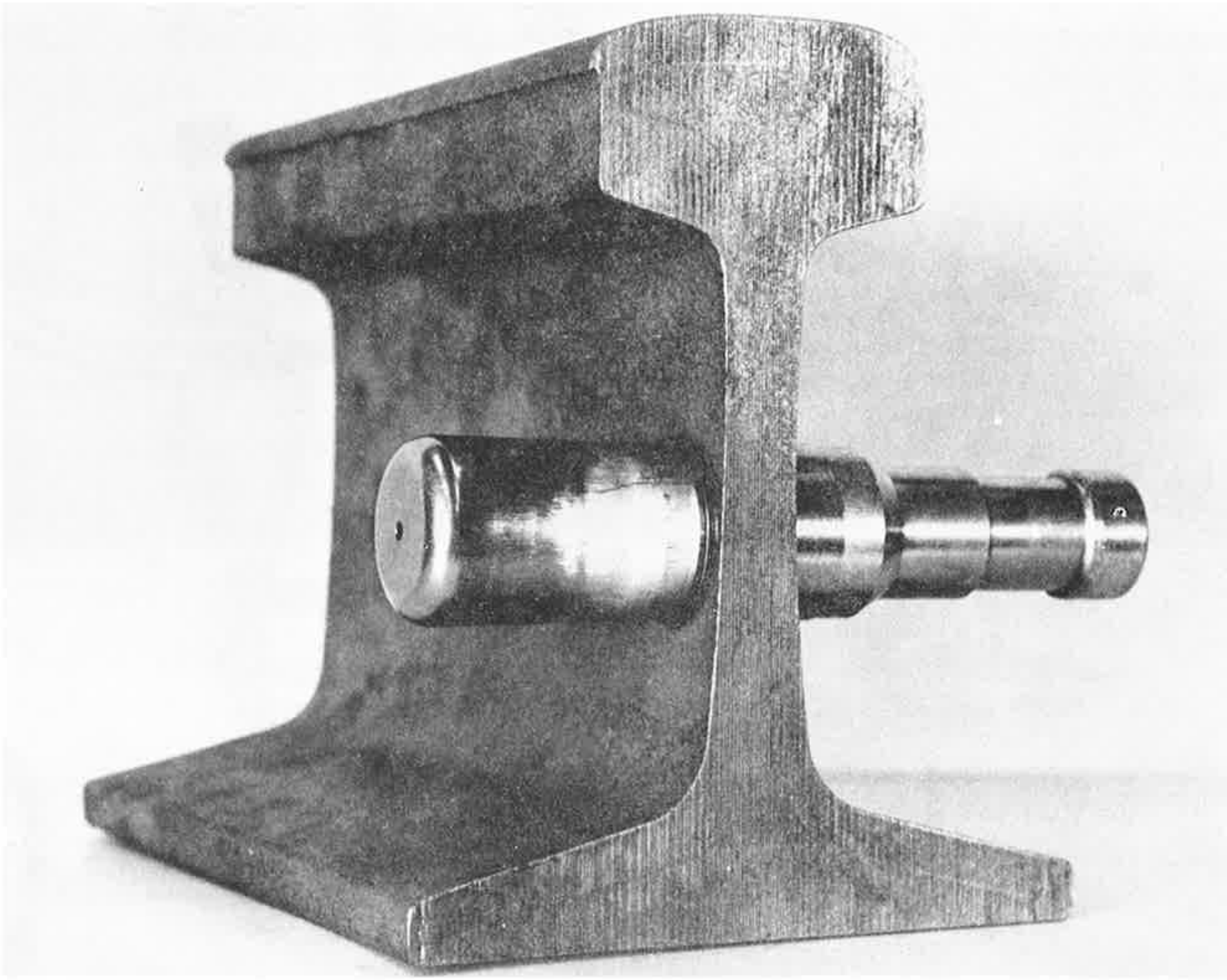

Figure 42.—Mandrel Inserted in Bolt Hole

The cold-expansion process was accomplished using two mandrels and one cold-expansion pull gun. One man placed a split sleeve on the mandrel and inserted the mandrel in the bolt-hole bore. The automatic chuck of the pull gun grasped the tang of the mandrel and drew the mandrel through the bore, the 0.055-inch diametrical interference between mandrel/ sleeve and bore developing the cold-expansion effect. The flare of the split sleeve (fig. 43) caused it to remain in the bore. As one operator removed the sleeve by using a single rap of a plastic-head hammer, the second man placed the other sleeve mandrel in the bore. Thus, the cold-expansion gun was operated nearly continuously at a rate one-third again as fast as the broach operation, due to the shorter stroke and slightly faster pull rate.

Union Pacific employed one man to deburr the hole edges after cold expansion and after the broach operation where only broaching was used.

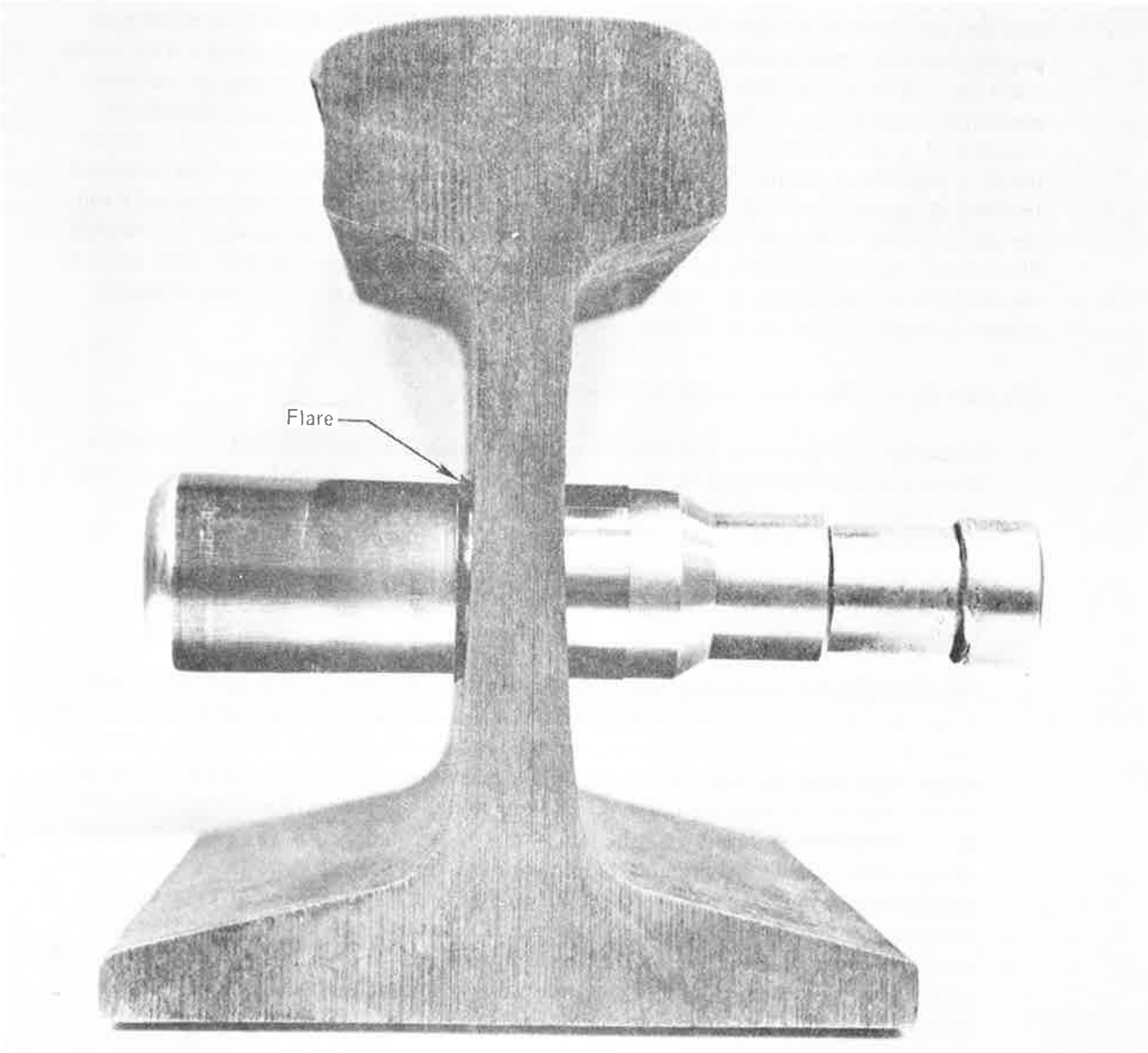

Figure 43.—Mandrel and Sleeve Properly Seated

The test site experiment demonstrated the facility with which the sleeve-cold-expansion process could be applied to railroad-rail bolt holes. Although various problems with equipment and the broach tooling did arise, the actual sleeve-cold-expansion process remained essentially troublefree. Cold-expansion mandrels jammed in holes five times during the working of approximately 6000 holes. Each time, the mandrel was removed by cautious use of a spike maul. In four cases, the problem was attributed to sleeve-dry-film lubricant removal or damage from oil or grit; the oil and grit being transferred to the mandrel from the gloves of the workman. In one case, the sleeve was placed on the mandrel incorrectly. When pull force was applied, the sleeve was forced to a spiral shape (fig. 44). This allowed the mandrel to contact the bore of the hole, causing metal pickup. The mandrel/sleeve system proved 99.996% problem-free.

The primary problem areas encountered were:

1. **Broaches**–The broaches fabricated for the site were designed for 1000 holes before sharpening, as anticipated by previous factory experience. Actual experience at the Nebraska site demonstrated that only 300 to 400 holes could be broached before sharpening was required. The primary cause of this reduction in broach life can be attributed to the grit-impregnated grease remaining in the bolt hole after cleaning and reaming. Hole variation and ovality did not permit the reaming operation to completely clean the hole.

2. **Pull-Gun Chucks, Broaching, and Cold Expanding**–The broach-pull-gun chuck was a frequent cause of delay, although the basic design of the chuck proved reliable. However, the cutting oil required by the broach tended to work into the chuck, carrying metal chips from the broach into the chuck assembly. Such chips caused the chuck to jam, and in one instance created failure of the chuck jaws. This occurred in spite of an air-blast line mounted on the gun barrel to blow chips out. The frequency of this problem was directly related to site ambient-temperature conditions. Cold temperatures (less than 40°F) caused the broach cutting oil to thicken, decreasing the efficiency of the air blast in removing residual oil and metal chips. During some mornings even colder temperatures were encountered (less than 35°F) and compressed-air lines would freeze, eliminating the air blast, and the chuck would jam before the operator realized that the air blast was frozen.

   The cold-expansion-gun chuck failures also were caused by thickening of the broach cutting oil. The oil remaining on the rail web from the broach operation, was extruded into the barrel of the cold-expansion pull gun, carrying chips from the broaching operation to the cold-expansion-pull-gun chuck. Again, the colder temperature increased the frequency of this problem. At mile 106.112, this condition caused failure of the chuck jaws, shutting down the cold-expansion operation until replacement jaws could be delivered to the site.

3. **Pull Guns, Broaching, and Cold Expanding**–The cold-expansion-pull-gun model used proved trouble-free throughout the experiment. The two broach pull guns were 12-inch-stroke units with modified barrels. The seal systems in these units did not withstand the high pull force required for the 1-5/16-inch broaches. The first gun

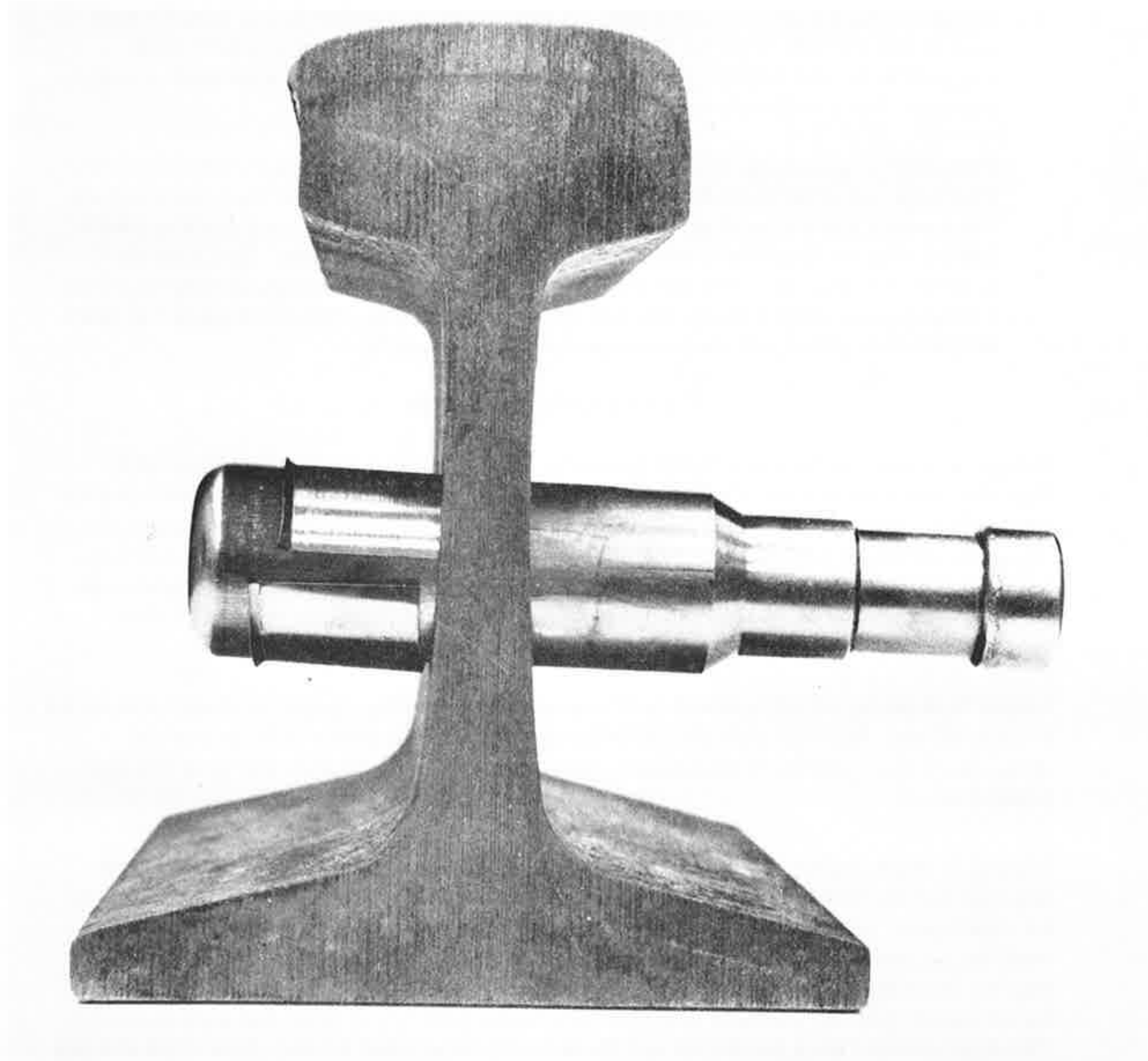

Figure 44.—Improper Sleeve Application

on site caused considerable delay until rebuilt with improved seals. A second gun, rebuilt prior to on-site delivery at the end of the first week of the test, proved trouble-free. However, throughout the entire experiment, both broach-gun units developed trouble with the device locking the gun nosepiece and barrel to the hydraulic portion of the gun. The locking device, an internal-expanding snapring, was too flexible to withstand the gun nosepiece impacting the rail as pull loads were first applied. One gun was wired together until larger snapring grooves were machined and heavier snap-rings were installed.

4. **Pneumatic Hydraulic Power Supplies**—A total of six pneumatic power supplies were used at the test site. Four of the units developed hydraulic leaks and were more susceptible to cold-weather power loss than were the two units of a different manufacturer. Two of the four units failed due to control-valve failure.

   Freeze-up of pneumatic power supply control air lines contributed to field problems. The freeze up of these units was caused by the control system, not the power system. The control systems used small (1/8-inch diameter) pressure lines and small balanced valving. Freeze up of these small orifices was the primary problem. The large air passages, 1/2-inch diameter and up, were not a problem. The standard compressed-air rail equipment did not freeze up, with the exception of the 1/4-inch-diameter air lines used to clear chips from the broach and pull guns (item 2).

4.5 PROCESS SUMMARY

The use of compressed-air-controlled hydraulic units at temperatures of less than 50°F does not appear to be a practical application. The energy transfer of air expansion causes a temperature drop in small metal parts (valves, etc.), to as much as 15°F. Compressed-air freeze up combined with the effect of temperature-thickened broach cutting oil created a large majority of the problems encountered during this test. Problems not associated with weather were limited to two hydraulic-fitting failures (fatigue) and the seals of the one broach pull gun.

Future field testing of rail-bolt-hole cold expansion will require equipment designed to avoid these problems. Mechanical or electric triggering of hydraulic power units is feasible. Also, use of small gasoline-engine-drive hydraulic units would eliminate the need for compressed air.

The use of track drilling equipment, possibly gang drills, designed for rapid and accurate alignment of the bolt holes should be considered, especially if cold weather operation is to be undertaken. Although drilling is slower than broaching, a greater variety of hole sizes could be accommodated with one drill size, permitting cold expansion of an increased number of holes in a given area of rail. For example, holes varying from 1-inch diameter to 1-3/8-inch diameter could be drilled to a common size (1-7/16 inch) and cold expanded. The elimination of thick cutting oil and the need for compressed air may show track drilling, especially two- or three-hole gang drills, as a strong competitor to broaching. This would be true only if the total rail crew was sized to the speed of the broach or drill operations. The Nebraska test crew used two joint cleanup crews. Where one broach gun was used, the cleanup crews could easily stay ahead of the broach crew. Where two broach guns were used (milepost 109 to 110), the broach crews were continually delayed by the cleanup crew. If proper track-drill equipment were to be provided, an efficient crew could be comprised of two cleanup units, two track-drill units or one gang-drill unit, and one cold-expansion unit.

5. CONCLUSIONS AND RECOMMENDATIONS

This information is contained in Volume III.

6. REFERENCES

1. *Broken Rails: A Major Cause of Train Accidents*, NTSB RSS-74-1, January 1974.

2. Wise, S., et al., *The Strength of Railroad Rails with Particular Reference to Rail Joints*, Proc. Inst. Mech. Engs., 174(9), pp. 371-407, 1960.

3. Wise, S., "Work Hardening Bolt Holes in Rail Ends", *Rail International*, pp. 863-865, October 1960.

4. Speakman, E.R., *Fatigue Life Improvement through Stress Coining Methods*, McDonnell Douglas paper 5506, June 1969.

5. Phillips, J.L., *Sleeve Coldworking Fastener Holes*, AFML-TR-74-10, Air Force Materials Laboratory, February 1974.

6. Mann, N.R., et al., *Methods for Statistical Analysis for Reliability and Life Data*, Wiley and Sons, New York NY, 1974.

7. Wagner, H., *Principles of Operational Research*, Prentice-Hall, Englewood Cliffs NJ, 1969.

APPENDIX A

TENSILE FATIGUE TEST RESULTS

Table A-1.—Non-Cold-Expanded and Cold-Expanded Tensile-Fatigue Results

Specimen no.	Hole size (in.)	Residual expansion (in.)		Coining (lbs x 1000)	Remarks	Net stress (ksi)	Cycles to failure
		Max	At test				
1A-4	1.00	0	0		No cold expansion	45	78,100
1A-5						40	85,280
1A-6						30	215,550
1A-7						35	221,530
1A-8	1.00	0	0		No cold expansion	27	332,940
1D-80	1.00	0	0	80	Coined	40	244,530
2D-120				120		40	362,620
3D-110				110		40	747,200
4D-270				270		35	327,400 [1]
4D-270	1.00	0	0	270	Coined	45	136,000 [2]
1.25A-1	1.25	0	0		No cold expansion	45	47,780
1.25A-2						35	154,550
1.25A-3						25	598,820
1.25A-4						30	204,510
1.25A-5	1.25	0	0		No cold expansion	27	436,830
1.25B-1	1.25	0.043	0.035		Sleeve expanded	45	130,170
1.25B-2						35	518,770
1.25B-3						30	3,496,000 [1]
1.25B-4						40	182,190
1.25B-5						37	196,000
1.25B-6						33	388,610
1.25B-7	1.25	0.043	0.035		Sleeve expanded	30	5,458,080 [1]
1.25C-1	1.25	0.053	0.045		Sleeve expanded	45	133,910
1.25C-2						40	103,280
1.25C-3						35	266,190
1.25C-4						33	543,740
1.25C-5	1.25	0.053	0.045		Sleeve expanded	30	2,797,900 [1]
1.25D-1	1.25	0.064	0.055		Sleeve expanded	45	78,400
1.25D-2						40	148,800
1.25D-3						35	286,650
1.25D-4						33	372,110
1.25D-5	1.25	0.064	0.055		Sleeve expanded	30	862,120
1.5A-1	1.50	0	0		No cold expansion	45	54,880
1.5A-2						35	139,460
1.5A-3						30	319,970
1.5A-4						40	87,420
1.5A-5	1.50	0	0		No cold expansion	25	3,386,910 [1]

[1] Test stopped without failure.
[2] Retest.

Table A-1.—Concluded

Specimen no.	Hole size (in.)	Residual expansion (in.) Max	Residual expansion (in.) At test	Coining (lbs x 1000)	Remarks	Net stress (ksi)	Cycles to failure
1.5B-4	1.50	0.033	0.022		Sleeve expanded	45	81,640
1.5B-5	↕	↕	↕		↕	35	293,040
1.5B-6	1.50	0.033	0.022		Sleeve expanded	30	258,260
1.5C-1	1.50	0.045	0.032		Sleeve expanded	45	74,900
1.5C-2	↕	↕	↕		↕	35	311,100
1.5C-3	1.50	0.045	0.032		Sleeve expanded	30	497,820
1.5D-1	1.50	0.055	0.044		Sleeve expanded	45	97,040
1.5D-2	↕	↕	↕		↕	35	304,580
1.5D-3	1.50	0.055	0.044		Sleeve expanded	30	589,000
1.25A-7	1.25	0	0		Clamped (no expansion)	35	280,000
1.25C-6	1.25	0.053	0.045		Clamped to prevent distortion	45	168,310
1.25C-7	1.25	0.053	0.045			35	1,387,260
1.25D-7	1.25	0.064	0.055		Clamped to prevent distortion	40	408,680
1.25F-1	1.25	0.025	0.005		Clamped to prevent distortion	45	22,720
1.25F-2	1.25	0.025	0.005			30	364,940

APPENDIX B
RAIL-FATIGUE TEST

Table B-1.—Rail-Fatigue Test S-N Curve Data

Specimen no.	Hole condition	Load level (kip)	Cycles	Remarks
3C-1	No cold expansion	140 [1]	235,940	Hole failure
3C-2		155 [1]	118,040	
3C-3		120 [1]	319,500	
3C-4		105	260,360	
3C-5		170	93,920	
3C-7	No cold expansion	80	1,134,310	Hole failure
3D-1	Cold expanded	140 [1]	460,360	First test—base failure
3D-1		140 [2]	1,012,170	Second test—no hole failure [3]
3D-2	Cold expanded	155	1,051,160	No failure
3D-3	---			No test
3D-4	Cold expanded	147 [1]	233,650	Cracked flange
3D-5		130 [1]	711,580	Cracked flange
3D-6		170	6,241,630	Hole failure
3D-7	Cold expanded	170	1,295,020	No failure

[1] Test using wood load pad.

[2] Load pad changed to steel for second test of 3D-1.

[3] Total cycles for 3D-1—1,472,530.

APPENDIX C
FATIGUE DATA

Table C-1.—Rail-Test-Matrix Fatigue Data

Specimen no.	Hole condition	Final crack length (in.)	Cycles	Remarks
Test: Nonfretted				
1A-1	Noncold expanded	0.28	67,060	Hole failure
1A-2	↕	0.27	97,900	↕
2A-1		0.32	138,200	
2A-2		0.28	242,000	
5A-1		0.27	133,290	
5A-2		0.26	135,000	
6A-1		0.28	132,730	
6A-4	Noncold expanded	0.27	105,310	Hole failure
1B-1	Cold expanded	—	643,820	Web failure
1B-2	↕	—	1,057,200	No failure
2B-1		—	1,083,130	↕
2B-2		—	1,514,500	
5B-1		—	1,047,090	
5B-2		—	2,147,480	No failure
6B-1		—	2,338,500	Head failure
6B-2	Cold expanded	—	1,025,000	No failure
Test: Fretted (load—8-kips tension load between holes)				
1A-3	Noncold expanded	2.20	96,550	Hole failure
1A-4	↕	2.70	88,730	↕
2A-3		0.28	96,300	
2A-4		0.29	105,330	
5A-6		0.32	111,220	
5A-8		0.32	106,250	
6A-5	Noncold expanded	0.28	103,410	Hole failure
6A-7	—	—	—	No test
1B-3	Cold expanded	—	254,460	Web failure
1B-4	↕	—	668,130	↕
2B-3		—	1,895,010	
2B-4		—	2,778,930	Web failure
5B-7		0.25	824,650	Hole failure
5B-8		0.25	2,726,880	↕
6B-7		0.25	654,480	
6B-8	Cold expanded	0.25	940,950	Hole failure

Note: Load level for all tests—170 kips.

Table C-1.—Concluded

Specimen no.	Hole treatment	Final crack length (in.)	Cycles	Remarks
Test: Precracked				
1A-2	Noncold expanded	0.70	7,240	Hole failure
2A 1		0.70	1,890	
2A-2	Noncold expanded	2.30	3,740	
5A-2	Cold expanded	0.80	294,450	
6A-1		0.77	2,455,570	Hole failure
6A-4	Cold expanded	0.53	416,670	Head to web failure
Test: Elongated				
1A-5	Noncold expanded	0.74	86,570	Hole failure
1A-6		0.40	132,260	
2A-5		0.27	91,450	
2A-6	Noncold-expanded	0.37	103,620	
1B-5	Cold expanded	0.28	1,864,063	Hole failure
1B-6		——	1,256,500	No failure
2B-5		0.27	484,550	Hole failure
2B-6	Cold expanded	0.30	1,348,230	Hole failure
Test: Four-hole specimen				
5A-3	Noncold expanded	0.32	153,090	Double crack (hole)
5A-4		0.28	92,050	Hole failure
6A-2		[1]	166,350	[1]
6A-3	Noncold expanded	0.28	118,000	Hole failure
5B-3	Cold expanded	——	1,026,300	No failure
5B-4		0.28	723,520	Hole failure
6B-3		——	1,034,430	No failure
6B-4	Cold expanded	——	1,136,660	No failure
Test: Crack-growth-rate specimen				
5A-5	Noncold expanded	0.30	129,830	Hole failure
5B-5	Cold expanded	——	1,277,000	Web failure

[1] Hole-initiated total failure.

Note: Load levels for all tests—170 kips.

APPENDIX D

REPORT OF INVENTIONS

The sleeve cold expansion process described in this report is not an innovation or discovery and is described in U.S. Patent 3,566,662, issued to the Boeing Company.

After a diligent review of the work performed under this contract, no innovation, discovery, improvement or invention was made.

110 Copies